Supporting Information

Searching for Small Molecules with an Atomic Sort

Brendan M. Duggan,[a,*] Reiko Cullum,[b] William Fenical,[b] Luis A. Amador,[c] Abimael D. Rodríguez,[c] and James J. La Clair,[d,*]

[a] Skaggs School of Pharmacy and Pharmaceutical Sciences, UC San Diego, 9500 Gilman Drive, La Jolla, California, 92093, United States.

[b] Center for Marine Biotechnology and Biomedicine, Scripps Institution of Oceanography, University of California at San Diego, La Jolla, California, 92093, United States

[c] Molecular Sciences Research Center, University of Puerto Rico, 1390 Ponce de León Avenue, San Juan, 00926, Puerto Rico

[d] Department of Chemistry and Biochemistry, UC San Diego, 9500 Gilman Drive, La Jolla, California, 92093, United States

Correspondence should be directed to bmduggan@ucsd.edu or jlaclair@ucsd.edu

Acknowledgments. This program was supported in part by funding from NIH Grant 1SC1GM086271-01A1 awarded to A.D.R., the Xenobe Research Institute to J. J. L., and NIH grant CA044848 to W.F.

Contents: **Page**

A. General Experimental Procedures. Chemical reagents were purchased from Acros, Fluka, Sigma-Aldrich, or TCI. Deuterated NMR solvents were purchased from Cambridge Isotope Laboratories. Analytical Thin Layer Chromatography (TLC) was performed on Silica Gel 60 F254 precoated glass plates (EM Sciences). Preparative TLC (pTLC) was conducted on Silica Gel 60 plates (EM Sciences). Visualization was achieved with UV light and/or an appropriate stain (I_2 on SiO_2, $KMnO_4$, bromocresol green, dinitrophenylhydrazine, ninhydrin, and ceric ammonium molybdate). Flash chromatography was carried out on Geduran Silica Gel 60 (40-63 mesh) from Analtech or EM Biosciences. Analytical HPLC was carried out using a HarmonySecure RP18 (250 x 4.6 mm i.d., 5 µm) column and was performed on an Agilent 1260 series system controller provided with an Agilent 1260 G1315D photodiode array detector with ChemStation software (Agilent). Optical rotations were measured in $CHCl_3$ with an Autopol IV automatic Polarimeter using a 10 mm microcell. Infrared and UV spectra were recorded using a Bruker Tensor 27 FTIR spectrometer and a Shimadzu UV-2401 PC UV-VIS recording spectrophotometer, respectively. NMR data were acquired with a Bruker DRX-500 spectrometer, Varian VS500 spectrometer, Varian VX500 spectrometer equipped with a Xsens Cold probe or a Bruker Avance III 600 equipped with a 1.7mm cryoprobe. Chemical shifts were referenced using the corresponding solvent signals (δ_H 7.26 and δ_C 77.00 for $CDCl_3$, δ_H 3.31 and δ_C 49.0 for CD_3OD). The NMR spectra were processed using Mestrenova (Mnova 11.0 Mestrelab Research) or TopSpin 3.0 (Bruker Biospin) software.

B. Microbial culturing. Strain CNB-382 was initially cultured in a 1 L volume using a seawater based A1 medium composed of 6 g of starch, 4 g of yeast, 2 g of glucose, 2 g of peptone, and 1 L seawater. After 7 days of cultivation, the broth was extracted with 1 L EtOAc, and the solvent was removed under vacuum to yield 30 mg of organic extract.

C. Purification of cyclomarin A. The organic extract (30 mg) was subjected to size exclusion chromatography (Sephadex LH-20) eluting with MeOH. Fractions containing cyclomarin A, as determined by NMR data, were then collected and fractionated by C-18 reversed-phase semi-prep HPLC (Phenomenex Luna C-18 column, 250 × 10 mm column, 5 *µ*m; 3 mL/min; 35% for 10 min and increase to 100% MeCN/H_2O over 60 min; UV detection at 210 nm) to yield cyclomarin A (1.8 mg).

Cyclomarin A. Colorless oil; $[\alpha]_D^{20}$ = -51.7° (*c* 0.48, $CHCl_3$); UV (MeOH) λ_{max} 222 (22,900), 287 (1000), and 293 (11,200); IR *v* (neat) 3400-3300, 3030, 2962, 2928, 2871, 1644, 1512, 1453, and 748 cm^{-1}; 1D and 2D-NMR data provided in Table S7; HR-FABMS obsd. $[M]^+$ *m/z* 1025.6062, calcd. 1025.6057 for $C_{56}H_{80}O_{10}N_9$; EI-MS (% relative intensity) 814 (1), 731 (1), 459 (2), 368 (3), 313 (4), 282 (16), 229 (35), 186 (21), 144 (69), 121 (100), and 116 (33).

D. Animal Material. The sponge *Plakortis halichondrioides* was collected in June 2006 during an underwater expedition near Mona Island, Puerto Rico. The sponge was frozen at -20 °C, and then lyophilized. A voucher specimen (IM06-19) is stored at the Molecular Sciences Research Center, University of Puerto Rico.

E. Purification of gracilioether L. The dry sponge *Plakortis halichondrioides* (32.4 g dry weight) was carefully cut into small chunks and blended in 1:1 $CHCl_3$/MeOH (2 × 100 L) at rt. After filtration, the crude extract was *concentrated in vacuo* to yield a brown thick paste (1.9 g). This extract was presented to flash column (38 mm ID × 200 mm height) washing with six rows of 15 test tubes with 150 mL of solvent (10 mL/tube) as given by row 1 (hexanes), row 2 (8:1 hexanes/EtOAc), row3 (4:1 hexanes/EtOAc), row 4 (2:1 hexanes/EtOAc), row 5 (1:1 hexanes/EtOAc) and row 6 (EtOAc). Each tube was explored by TLC analysis and tube 10 in row 5 displayed the targeted peaks. This was then subjected twice to pTLC first with 1:1 hexanes/EtOAc then 1:1 hexanes/acetone to deliver 1.2 mg of gracilioether L.

Gracilioether L. Colorless oil; $[\alpha]_D^{20}$ = -89.2 (*c* 0.05, CH_3OH); UV (CH_3OH) λ_{max} (log ε) 286 (2.74), 243 (2.17), 205 (2.42) nm; 1D and 2D-NMR data provided in Table S11; HR-ESI-MS *m/z* calcd. for $C_{21}H_{32}O_4$ $[M+Na]^+$: *m/z* 371.2198, found 371.2193.

F. HSQC database. Publicly available ^1H-^{13}C HSQC spectra were downloaded from HMDB (ww.hmdb.ca) and BMRB (bmrb.wisc.edu/metabolomics). Chemical shift referencing of the spectra was not modified after downloading. Chemical shifts were extracted from the peak lists in the downloaded data using perl and shell scripts and used without further modification. Precision of the chemical shifts varies depending on the data source. Plotting the chemical shift data enabled visual identification of outliers, which were inspected manually using TopSpin. Peaks picked on noise, artifacts, or two bond correlations were removed. Chemical shifts for common solvents were obtained from Tables 1 and 2 in Gottlieb, H. E.; Kotyar, V.W.; Nudelman, A. *J. Org. Chem*. **1997**, *62*, 7512-7515. In-house ^1H-^{13}C HSQC spectra of standards cholesteryl acetate, sucrose, o-dichlorobenzene, ethylbenzene, strychnine and streptomycin and from recent projects (see references: (a) Mehrotra S.; Duggan, B. M. Tello-Aburto, R.; Newar, T. D.; Gerwick, W. H.; Murray, T. F.; Maio, W. A. *J. Nat Prod.* **2014**, *77*, 2553-2260; (b) Kleigrewe, K.; Almaliti, J.; Tian, I. Y.; Kinnel, R. B.; Korobeynikov, A.; Monroe, E. A.; Duggan, B. M.; Di Marzo, V.; Sherman, D. H.; Dorrestein, P. C.; Gerwick, L.; Gerwick, W. H. *J. Nat. Prod.* **2015**, *78*, 1671-1682; (c) Wang, X.; Duggan, B. M., Molinski, T. F. *J. Am. Chem. Soc.* **2015**, *137*, 12343-12351; (d) White, A. R.; Duggan, B. M.; Tsai, S. C.; Vanderwal, C. D. *Org Lett.* **2016**, *18*, 1124-1127; (e) Carling, C. J.; Olejniczak, J.; Foucault-Collet, A.; Collet, G.; Viger, M. L.; Huu, V. A.; Duggan, B. M.; Almutairi, A. *Chem. Sci.* **2016**, *7*, 2392-2398; (f) Li, Z. R.; Li, J.; Gu, J. P.; Lai, J. Y.; Duggan, B. M.; Zhang, W. P.; Li, Z. L.; Li, Y. X.; Tong, R. B.; Xu, Y.; Lin, D. H.; Moore, B. S.; Qian, P. Y. *Nat. Chem. Biol.* **2016**, *12*, 773-775) were processed with TopSpin 3.6. Spectra were referenced to internal TMS or residual solvent. Peaks were picked automatically at a high threshold with the interpolation type set to "parabolic". The threshold was then reduced and additional weak peaks were added. Noise, artifacts and two bond correlations were removed. Peaks picked on individual lines in multiplets were combined to a single peak. Peaks from all four data sources were combined to give the final database. A subset of the database that excluded aldehydes was fitted to a straight line to obtain the equation δ_C= 16.9989 δ_H + 1.06803. Including aldehydes gave a poor fit. Taking every point in the database the difference between the experimental δ_C and that calculated from the fitted line was determined and the standard deviation of these differences calculated. In the entire database only six points were found to fall more than four standard deviations (99.99% confidence limit) from the line.

G. Chemical shift extraction and distance scoring. Samples for profiling were dissolved in 50µl of methanol-d_4 and transferred to 1.7mm NMR tubes. ^1H-^{13}C HSQC spectra were collected using a 1.7mm microcryoprobe and processed using TopSpin 3.6. Peaks were picked as described above for the database spectra. Peaks more than four standard deviations from the line fitted to the database were flagged. The distance score was calculated as

$$\text{distance score} = \{ [(\delta_{H,query} - \delta_{H,db}) / \text{range } \delta_H]^2 + [(\delta_{C,query} - \delta_{C,db}) / \text{range } \delta_C]^2 \}^{½}$$

where δ_H is the proton chemical shift, δ_c is the carbon chemical shift, the subscript "query" indicates the query peak and "db" a peak in the database, and range is the difference between the minimum and maximum chemical shifts of the indicated nucleus observed in the database. For each query peak the distance score was calculated for all peaks in the database and the minimum value reported.

Table S1. Atomic novelty scores for bromophycolide A

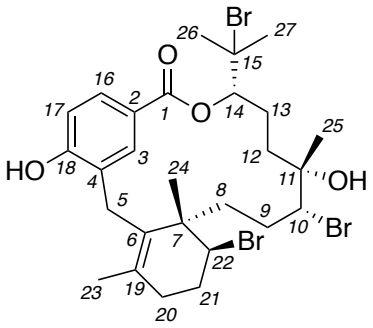

peak[1]	position[2]	δ_H	δ_C	distance
14	14	4.69	81.4	0.47%
16	22	4.56	61.8	0.36%
1	3	7.99	132.1	0.35%
12	16	7.74	130.2	0.25%
18	5	3.47	30.0	0.25%
19	20	2.07	34.0	0.23%
5	12	1.17	36.1	0.20%
13	17	6.88	115.4	0.20%
3	8	1.93	38.8	0.19%
21	21	2.32	31.4	0.15%
4	9	1.80	29.5	0.14%
23	9	2.08	29.4	0.13%
17	5	3.30	30.0	0.12%
11	24	1.30	26.2	0.12%
7	27	1.81	31.7	0.12%
8	23	1.42	20.9	0.09%
2	12	1.64	36.1	0.08%
10	26	1.83	31.0	0.07%
6	8	1.36	38.8	0.06%
15	10	3.40	72.3	0.03%
9	25	1.28	33.2	0.02%
20	20	2.35	34.0	0.02%
22	13	2.12	29.3	0.02%

[1] Peak is a number that identifies the order that the peaks were abstracted from the raw data.

[2] Position identifies the atom number given by Kubanek, J.; Prusak, A. C.; Snell, T. W.; Giese, R. A.; Hardcastle, K. I.; Fairchild, C. R.; Aalbersberg, W.; Raventos-Suarez, C.; Hay, M. E. *Org. Lett.* **2005**, *7*, 5261-5264.

Table S2. Atomic novelty scores for strychnine

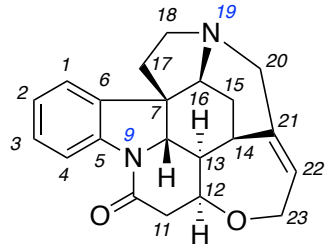

peak[1]	position[2]	δ_H	δ_C	distance[3]
2	4	8.10	116.3	1.89%
14	13	1.27	48.2	1.01%
3	22	5.90	127.4	0.60%
6	20	2.72	52.6	0.49%
7	20	3.70	52.6	0.43%
19	12	4.28	77.6	0.42%
12	18	3.20	50.4	0.37%
16	17	1.89	42.8	0.37%
21	16	3.95	60.2	0.30%
15	14	3.14	31.6	0.29%
9	15	2.37	27.0	0.27%
20	8	3.85	60.1	0.26%
13	18	2.87	50.4	0.26%
8	11	2.65	42.5	0.17%
17	23	4.07	64.5	0.15%
11	11	3.11	42.4	0.15%
18	23	4.14	64.6	0.13%
1	3	7.26	128.5	0.12%
10	15	1.47	26.8	0.08%
5	1	7.16	122.4	0.07%
4	2	7.10	124.2	0.03%

[1] Peak is a number that identifies the order that the peaks were abstracted from the raw data.

[2] Position identifies the atom number as given by Verpoorte R. *J. Pharm Sci.* **1980**, 69, 865-866.

[3] The strychnine data was removed from the database before calculating these distance scores.

Table S3. Atomic novelty scores for brusatol

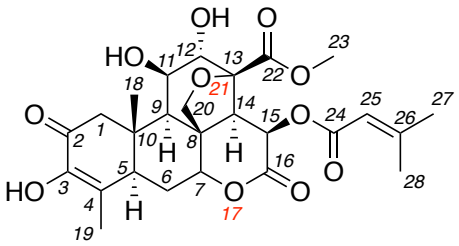

peak[1]	position[2]	δ_H	δ_C	distance
2	7	4.91	84.5	0.91%
11	19	1.84	13.1	0.54%
9	28	2.17	20.2	0.53%
16	1	2.84	49.8	0.35%
17	1	2.53	49.8	0.33%
18	6	2.30	29.7	0.30%
15	5	2.97	42.9	0.26%
5	14	3.80	52.8	0.21%
4	11,15	4.17	72.6	0.16%
10	27	1.94	27.2	0.12%
13	20	4.69	74.2	0.08%
14	20	3.71	74.2	0.07%
8	6	1.87	29.8	0.07%
12	18	1.37	15.3	0.07%
3	25	5.68	115.6	0.05%
1	12	4.20	76.2	0.05%
6	23	3.72	52.7	0.03%
19	9	2.21	42.1	0.02%

[1] Peak is a number that identifies the order that the peaks were abstracted from the raw data.

[2] Position identifies the atom number as given by Hagigaya, Y.; Konda, Y.; Iguchi, M.; Onda, M.; Li, X.; Wu, L.; Li, S.; Sun, X. *J. Nat. Prod.* **1989**, *52*, 740-748.

Table S4. Atomic novelty scores for paclitaxel

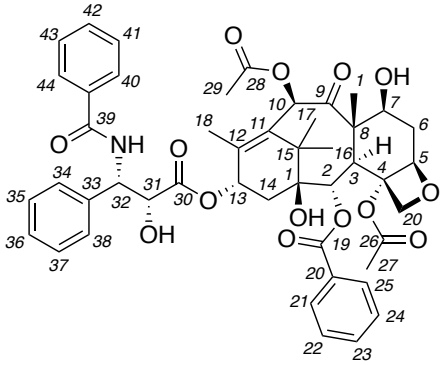

peak[1]	position[2]	δ_H	δ_C	distance
14	10	6.45	76.5	1.76%
12	32	5.64	57.5	1.73%
11	13	6.16	71.9	1.12%
27	5	5.00	85.6	0.65%
19	29	2.17	20.5	0.48%
26	2	5.65	75.9	0.46%
20	27	2.36	22.9	0.37%
28	3	3.83	47.6	0.36%
21	19	1.66	10.1	0.31%
8	21,25	8.11	130.9	0.24%
1	23	7.67	134.3	0.19%
7	34,38	7.49	128.2	0.18%
5	41,43	7.47	129.3	0.18%
3	42	7.55	132.6	0.17%
2	36	7.29	128.7	0.16%
15	27	4.19	77.2	0.15%
22	6	2.47	37.2	0.14%
16	16	1.15	22.0	0.14%
6	35, 37	7.42	129.4	0.13%
9	40, 44	7.86	128.2	0.13%
4	22, 24	7.58	129.4	0.10%
13	31	4.74	74.6	0.07%
18	18	1.91	14.4	0.06%
24	6	1.81	37.2	0.03%
17	17	1.16	26.6	0.03%
25	14	1.96	36.2	0.02%
23	14	2.23	36.3	0.01%
10	7	4.32	72.0	0.01%

[1] Peak is a number that identifies the order that the peaks were abstracted from the raw data.

[2] Position identifies the atom number as given by Chmurny, G. N.; Hilton, B. D.; Brobst, S.; Look, S. A.; Witherup, K. M.; Beutler, J. A. *J. Nat. Prod.* **1982**, *55*, 414-423.

Table S5. Atomic novelty scores for the CNB-982 extract.[1]

peak[2]	δ_H	δ_C	distance
289	-0.91	32.4	13.74%
95	6.15	145.4	2.53%
94	5.97	147.4	2.36%
2	7.27	147.9	2.01%
270	0.80	3.9	1.91%
192	2.58	67.9	1.60%
146	5.33	89.5	1.51%
191	2.70	67.9	1.42%
7	8.23	134.0	1.36%
6	8.22	122.4	1.28%
259	0.75	7.6	1.28%
60	0.34	15.4	1.28%
194	2.97	67.6	1.15%
274	1.05	42.5	1.14%
260	0.85	5.0	1.13%
287	5.33	59.9	1.13%
271	0.77	7.8	1.11%
137	5.11	126.6	1.10%
203	2.62	25.4	1.00%
58	4.93	84.4	1.00%
288	5.03	126.2	0.98%
275	1.10	42.0	0.97%
122	7.79	114.3	0.95%
9	6.61	98.0	0.90%
280	4.72	95.1	0.89%
149	4.59	64.5	0.73%
40	5.00	57.3	0.71%
139	5.21	113.7	0.71%
181	4.01	45.0	0.71%
151	4.54	57.1	0.69%
43	4.74	66.0	0.69%
145	5.26	70.9	0.66%
272	0.42	16.7	0.66%
169	3.25	78.5	0.64%
134	6.88	110.6	0.63%
91	5.12	77.9	0.60%
190	3.60	46.1	0.59%
193	2.91	67.6	0.56%
143	5.20	76.7	0.56%
142	5.26	73.7	0.55%
153	4.35	54.9	0.54%
170	3.24	80.9	0.50%

183	4.02	51.4	0.50%
97	6.64	131.6	0.49%
261	1.00	6.9	0.48%
158	3.94	54.1	0.47%
176	3.39	43.2	0.47%
35	4.53	59.1	0.47%
140	5.00	76.8	0.46%
157	3.91	60.5	0.46%
215	1.68	43.4	0.45%
232	2.01	23.3	0.45%
22	4.40	51.5	0.43%
132	6.71	111.5	0.43%
217	1.77	41.9	0.43%
279	5.02	111.7	0.43%
163	4.31	57.0	0.43%
133	6.56	111.4	0.42%
67	2.03	23.0	0.41%
104	7.04	131.9	0.41%
286	1.10	29.5	0.40%
167	4.01	84.3	0.40%
99	7.78	132.5	0.39%
29	2.04	13.8	0.39%
150	4.46	68.8	0.39%
196	2.82	45.9	0.38%
79	2.50	29.6	0.37%
189	3.42	44.3	0.36%
184	3.50	48.9	0.36%
101	8.02	130.4	0.36%
236	1.19	25.7	0.35%
266	0.92	33.7	0.35%
156	4.00	59.8	0.34%
36	3.37	45.6	0.33%
144	5.34	73.2	0.33%
177	3.37	41.9	0.33%
100	7.85	132.2	0.33%
27	2.08	22.2	0.33%
126	7.46	112.7	0.32%
221	1.27	40.5	0.32%
218	1.87	42.1	0.32%
209	2.32	31.0	0.31%
206	2.81	32.8	0.31%
257	0.96	17.6	0.31%
123	7.58	119.5	0.31%
20	1.17	28.8	0.31%

108	7.21	123.1	0.30%
49	4.06	59.8	0.29%
242	0.96	21.9	0.29%
70	2.32	29.2	0.29%
175	4.18	51.8	0.29%
72	3.54	45.8	0.28%
45	1.98	15.1	0.28%
119	7.35	126.1	0.27%
141	4.84	73.7	0.27%
103	7.91	131.3	0.27%
131	6.66	116.0	0.27%
222	1.12	40.4	0.26%
44	3.25	58.5	0.26%
246	1.14	17.3	0.26%
121	7.90	122.3	0.26%
201	2.49	39.0	0.25%
148	4.79	58.9	0.25%
211	2.06	39.3	0.25%
179	3.74	46.7	0.25%
262	0.67	16.6	0.25%
224	1.25	34.3	0.24%
216	1.68	42.6	0.24%
164	4.42	56.9	0.24%
31	1.13	24.5	0.24%
83	4.26	60.0	0.24%
52	4.60	46.7	0.23%
17	5.35	130.6	0.23%
278	2.03	42.2	0.23%
250	1.07	15.2	0.23%
225	1.23	32.9	0.23%
200	2.55	38.2	0.23%
178	3.51	43.2	0.23%
248	1.18	18.8	0.22%
159	3.90	54.5	0.22%
74	4.19	59.7	0.22%
16	7.28	130.1	0.22%
63	1.93	23.0	0.22%
208	2.30	28.8	0.22%
65	4.44	57.4	0.22%
256	1.01	15.4	0.21%
118	7.46	129.2	0.21%
82	2.88	29.9	0.21%
284	1.19	28.3	0.21%
10	7.13	122.4	0.21%

76	0.90	19.7	0.21%
152	4.65	57.9	0.21%
155	4.26	59.0	0.20%
239	1.06	22.3	0.20%
102	8.06	129.4	0.20%
129	6.75	115.7	0.20%
13	7.24	129.1	0.20%
277	1.43	38.2	0.20%
75	4.03	61.2	0.19%
172	3.54	62.7	0.19%
138	5.38	131.2	0.19%
96	6.60	134.1	0.19%
42	3.25	55.7	0.19%
204	2.77	36.5	0.19%
213	2.35	29.8	0.19%
77	1.64	19.4	0.19%
90	3.34	56.0	0.19%
173	3.59	62.1	0.19%
105	7.03	130.6	0.19%
240	1.00	20.8	0.18%
214	2.29	23.5	0.18%
212	2.05	28.8	0.18%
258	1.02	21.9	0.18%
241	0.97	20.1	0.18%
66	1.11	19.0	0.18%
1	7.22	131.3	0.18%
41	1.74	28.1	0.17%
86	4.07	61.0	0.17%
46	1.12	18.5	0.17%
81	1.68	24.7	0.17%
11	7.29	127.6	0.17%
54	2.01	28.8	0.17%
220	1.57	32.4	0.17%
26	4.36	57.6	0.17%
254	1.00	18.1	0.17%
182	4.10	46.6	0.17%
116	7.36	128.0	0.16%
180	3.83	45.0	0.16%
68	3.64	71.2	0.16%
264	1.69	16.1	0.16%
273	2.16	44.0	0.16%
263	0.86	9.9	0.16%
276	1.91	39.1	0.16%
38	1.17	25.6	0.15%

78	1.81	25.9	0.15%
223	1.18	40.0	0.15%
135	7.04	120.3	0.15%
154	4.23	57.2	0.15%
186	3.03	37.4	0.15%
28	1.91	19.9	0.14%
47	3.04	39.9	0.14%
19	1.60	26.6	0.14%
53	2.19	36.3	0.14%
109	7.23	124.1	0.14%
269	0.86	10.9	0.14%
249	1.17	19.9	0.14%
197	2.67	40.3	0.14%
107	7.01	119.7	0.14%
185	3.09	37.4	0.14%
219	1.82	42.1	0.14%
265	1.12	32.1	0.14%
5	7.10	125.3	0.14%
252	1.00	23.1	0.14%
238	1.03	23.8	0.14%
188	3.19	40.7	0.13%
136	5.77	125.1	0.13%
244	1.09	18.6	0.13%
187	2.99	40.6	0.13%
117	7.40	129.6	0.13%
127	7.33	112.0	0.13%
199	2.71	39.1	0.13%
8	7.30	128.2	0.13%
243	0.96	23.0	0.13%
147	5.18	61.2	0.13%
165	4.09	71.4	0.13%
71	1.12	19.6	0.12%
24	1.31	20.7	0.12%
115	7.18	127.0	0.12%
62	0.89	22.8	0.12%
233	1.74	25.8	0.12%
106	7.09	122.3	0.12%
21	1.35	20.7	0.12%
285	1.53	28.9	0.12%
64	1.52	39.1	0.11%
268	0.91	11.0	0.11%
33	1.44	25.1	0.11%
15	7.23	127.6	0.11%
3	7.24	130.0	0.11%

112	7.28	130.9	0.11%
229	1.68	26.2	0.11%
255	1.03	15.3	0.11%
80	4.13	54.3	0.11%
125	7.50	114.7	0.11%
227	1.52	33.3	0.11%
51	1.14	18.9	0.11%
230	1.88	25.5	0.11%
128	6.86	116.1	0.10%
210	1.98	33.3	0.10%
61	2.68	30.3	0.10%
231	1.86	25.0	0.10%
4	7.35	129.2	0.10%
195	2.88	45.9	0.10%
228	1.35	30.4	0.10%
89	3.31	49.0	0.10%
120	7.26	124.8	0.10%
162	3.78	61.2	0.10%
92	3.59	41.9	0.10%
32	1.91	22.3	0.09%
88	3.51	46.1	0.09%
198	2.75	40.1	0.09%
205	2.81	29.7	0.09%
48	2.67	37.8	0.09%
160	3.84	56.0	0.09%
237	1.14	20.9	0.09%
124	7.54	120.0	0.08%
171	3.68	64.4	0.08%
59	0.96	19.1	0.08%
37	2.03	27.9	0.08%
207	2.32	34.7	0.08%
114	7.18	131.0	0.08%
34	1.91	23.3	0.08%
18	1.32	25.1	0.08%
130	6.71	115.9	0.08%
57	1.15	18.4	0.07%
55	2.16	36.7	0.07%
30	2.09	29.1	0.07%
84	1.50	22.8	0.07%
235	1.45	20.6	0.07%
87	0.93	12.3	0.06%
12	7.26	128.9	0.06%
282	1.33	30.0	0.06%
39	1.32	23.4	0.06%

161	3.85	56.7	0.06%
110	7.32	128.1	0.06%
234	1.38	15.4	0.06%
247	1.05	19.0	0.06%
98	7.76	126.7	0.06%
202	2.43	40.1	0.05%
25	2.27	34.8	0.05%
281	4.09	65.4	0.05%
168	3.53	72.3	0.05%
251	0.93	16.4	0.05%
283	1.21	29.1	0.05%
56	1.93	29.2	0.05%
166	3.94	72.6	0.04%
245	1.07	17.8	0.04%
93	1.29	30.5	0.04%
226	1.41	31.5	0.04%
113	7.24	130.8	0.03%
253	0.87	19.9	0.03%
14	7.21	124.6	0.03%
50	1.29	32.8	0.03%
69	1.80	22.5	0.03%
85	3.22	58.1	0.03%
73	3.16	37.9	0.02%
174	3.74	64.0	0.02%
267	0.89	14.3	0.01%
111	7.29	129.2	0.01%
23	1.60	25.9	0.01%

[1] Green shading denotes the top five peaks observed in the pure cyclomarin A spectrum (Table S6). These peaks were identified after the pure material was obtained to emphasize that many of the most highly scoring peaks in the mixture came from a single compound, namely cyclomarin A.

[2] Peak is a number that identifies the order that the peaks were abstracted from the raw data.

Table S6. Atomic novelty scores for cyclomarin A

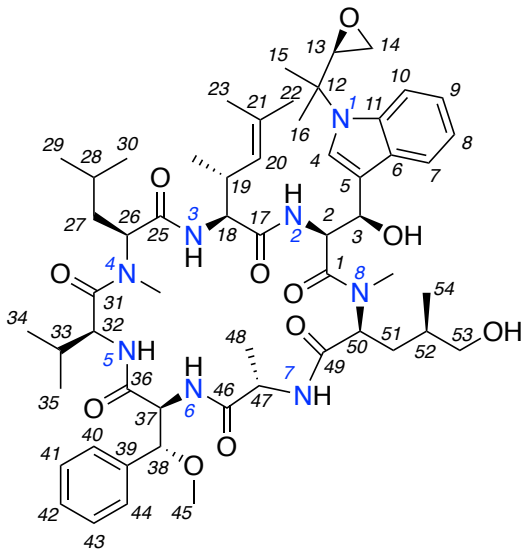

peak[1]	position[2]	δ_H	δ_C	distance
41	51β	-0.92	32.4	13.64%
7	53β	2.58	67.9	1.62%
34	53α	2.71	67.9	1.37%
12	54	0.35	15.6	1.24%
29	26	5.34	61.7	1.18%
27	20	5.03	126.3	0.99%
4	38	4.97	84.5	0.99%
25	7	7.79	114.3	0.91%
32	32	4.54	57.1	0.69%
28	3	5.26	70.8	0.64%
6	37	4.99	57.4	0.62%
31	18	4.52	59.1	0.54%
33	47	4.39	51.4	0.43%
20	NMe-8	2.50	27.7	0.39%
36	33	2.31	31.1	0.36%
13	14β	2.83	46.1	0.36%
24	10	7.91	122.5	0.29%
15	13	3.25	58.5	0.26%
11	29	1.07	22.4	0.23%
30	50	4.79	58.0	0.22%
40	52	1.23	33.1	0.20%
18	NMe-4	2.88	28.1	0.20%
5	2	4.65	58.0	0.19%
1	8	7.13	122.3	0.19%
45	23	1.61	22.7	0.18%
22	15	1.69	24.8	0.17%

2	9	7.04	120.2	0.17%
16	34	0.98	20.1	0.15%
19	22	1.81	26.0	0.15%
38	48	1.00	20.8	0.15%
37	35	1.12	19.5	0.13%
14	19	2.77	36.6	0.13%
17	30	1.04	23.9	0.11%
23	16	1.50	22.7	0.11%
43	41,43	7.29	129.3	0.09%
9	27β	1.14	40.1	0.08%
26	40,44	7.32	128.0	0.07%
10	27α	2.44	40.1	0.07%
35	14α	2.89	46.1	0.06%
8	51α	1.57	32.4	0.06%
44	28	1.77	24.9	0.05%
39	24	0.96	19.1	0.04%
21	45	3.22	58.1	0.04%
3	4	7.21	124.8	0.03%
42	42	7.26	129.1	0.02%

[1] Peak is a number that identifies the order that the peaks were abstracted from the raw data.

[2] Position identifies the atom number as given in Renner, M. K.; Shen, Y.-C.; Cheng, X.-C.; Jensen, P. R.; Frankmolle, W.; Kaufmann, C. A.; Fenical, W.; Lobkovsky, E.; Clardy, J. *J. Am. Chem. Soc.* **1999**, *121*, 11273-11276.

Table S7. NMR spectral data for cyclomarin A in CD_3OD

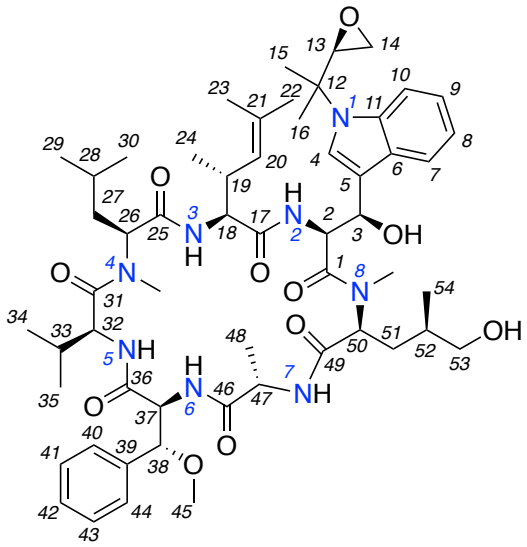

cyclomarin A

Position	δ_C, Type	δ_H, mult (*J* in Hz)	^{1}H-^{1}H COSY	^{1}H-^{13}C HMBC[1]
1	171.8, C	-		
2	58.0,CH	4.65, d (9.3)	3	1,3,5,17
3	70.8,CH	5.26, d (9.3)	2	2,4,5,6
4	124.8,CH	7.21 s		2,3,5,6,10w,11
5	114.3,C	-		
6	127.5,C	-		
7	122.5, CH	7.91 d (7.9)	8	6,9
8	122.3,CH	7.13, t (7.5)	7,9	7w,10,11
9	120.2, CH	7.04, t (7.6)	8,10	6,7
10	114.3,CH	7.79, d (8.5)	9	7,8,11
11	135.2, C	-		
12	57.4,C	-		
13	58.5,CH	3.25 dd (2.6, 4.1)	14α,14β	14
14α	46.1,CH_2	2.89 m	13,14β	13
14β		2.83 dd (2.7, 4.7)	13,14α	
15	24.8,CH_3	1.69 s	16	
16	22.7,CH_3	1.50 s	15	
17	172.3,C	-		
18	59.1,CH	4.52 d (10.0)	19	17,19,20,25
19	36.6,CH	2.77 dt (6.5,10.2)	18,20,24	17,18,20,21
20	126.3,CH	5.03 d (9.8)	19,22,23	18,19,22,23
21	134.5,C	-		
22	26.0,CH_3	1.81 d (0.4)	20	20,21,23
23	22.7,CH_3	1.61 d (0.3)	20	20,21,22
24	19.1,CH_3	0.96 d (6.7)	19	18,19,21
25	170.0,C	-		

26	61.7,CH	5.34 dd (3.0,11.3)	27α,27β	23,25,27α,27β,31,NMe-4
27α	40.1,CH_2	2.44 ddd (4.0, 11.3, 13.1)	26,27β,28	26,28,29,30
27β		1.14 m	26,27α,28	26,28,29,30
28	24.9,CH	1.77 m	27α,27β,29,30	26,27α,27β,29,30
29	22.4,CH_3	1.07 d (6.6)	28	23,27,30
30	23.9,CH_3	1.04 d (6.6)	28	23,27,29
31	173.2,C	-		
32	57.1,CH	4.54 d (9.5)	33	31,33,34,36
33	31.1,CH	2.31 ddt (13.3, 10.1, 6.7)	32,34,35	32,35
34	20.1,CH_3	0.98 (d, 6.7)	33	32,33,35
35	19.5,CH_3	1.12 (d, 6.6)	33	32,33,34
36	171.6,C	-		
37	57.4,CH	4.99 d (3.4)	38	36,38,45w,46
38	84.5,CH	4.97 d (3.6)	37	36,37,39,40,44
39	137.5	-		
40	128.0,CH	7.32 d (6.5)	41	38,44
41	129.3,CH	7.29 t (6.6)	40,42	39,40
42	129.1,CH	7.26 t (6.8)	41,43	39,40,44
43	129.3,CH	7.29 t (6.6)	42,44	39,44
44	128.0,CH	7.32 d (6.5)	43	38,40
45	58.1, CH_3	3.22 s		38
46	172.7,C	-		
47	51.4, CH	4.39 q (7.2)	48	46,48,49
48	20.8, CH_3	1.00 d (7.2)	47	46,47
49	170.7,C	-		
50	58.0,CH	4.79 dd (2.8, 12.4)	51α,51β	1,49,52,NMe-8
51α	32.4,CH_2	1.57 m	50,51β,52	49,50
51β		-0.92 m	50,51α,52	49,50,NMe-8
52	33.1,CH	1.23 m	51α,51β,54,53	54
53α	67.9,CH_2	2.71 dd (6.1, 10.6)	52,53β	52,54
53β		2.58 dd (7.3, 10.6)	52,53α	52,54
54	15.6,CH_3	0.35 d (6.7)	52	51,52,54
NMe-4	28.1,CH_3	2.88 s		26,31
NMe-8	27.7,CH_3	2.50 s		1,3w,50

[1] w denotes a weak cross peak

Table S8. Tabulation of the atomic novelty scores for the IM06-19 extract[1]

peak[2]	δ_H	δ_C	distance
159	6.43	148.3	3.30%
1	6.68	154.9	3.13%
153	5.03	134.5	1.62%
3	5.08	134.7	1.19%
152	6.48	142.2	1.13%
161	5.55	125.7	1.09%
146	0.80	8.1	0.93%
169	5.32	135.2	0.87%
86	0.84	29.5	0.85%
165	5.36	133.6	0.79%
13	3.66	51.1	0.75%
141	0.85	8.0	0.66%
5	4.58	78.1	0.63%
163	5.04	125.4	0.63%
4	5.42	133.7	0.61%
151	7.13	153.2	0.53%
68	1.75	39.1	0.47%
95	0.83	9.0	0.43%
8	4.85	83.9	0.42%
104	0.96	8.1	0.40%
160	6.24	129.8	0.39%
157	5.16	73.0	0.38%
66	0.87	33.9	0.38%
154	4.51	78.7	0.38%
113	1.18	21.9	0.37%
166	5.35	130.9	0.36%
176	1.86	45.6	0.35%
122	1.23	34.6	0.34%
188	1.63	34.1	0.34%
175	1.75	45.8	0.33%
186	1.89	43.8	0.33%
124	1.57	33.9	0.33%
144	1.18	12.6	0.32%
100	0.96	13.1	0.31%
14	2.13	45.9	0.31%
69	0.96	10.5	0.30%
106	1.09	12.3	0.30%
2	6.06	132.4	0.29%
136	2.27	19.5	0.29%
21	1.26	35.8	0.29%
61	1.27	36.7	0.28%
36	0.96	9.7	0.28%

35	1.03	12.2	0.28%
116	0.88	9.2	0.27%
102	1.22	40.1	0.26%
96	0.94	26.2	0.26%
182	1.54	41.3	0.26%
184	1.83	42.0	0.26%
173	3.70	52.2	0.26%
183	1.62	41.9	0.25%
67	0.83	22.1	0.23%
105	2.08	24.3	0.23%
115	1.21	22.3	0.23%
50	0.82	9.7	0.23%
17	2.00	37.4	0.23%
148	0.98	14.7	0.23%
180	2.48	38.3	0.22%
125	1.19	26.2	0.22%
46	1.12	38.2	0.22%
158	4.53	63.7	0.22%
37	1.69	37.9	0.22%
19	0.97	20.6	0.22%
133	1.19	29.5	0.21%
30	1.58	31.9	0.21%
71	1.24	36.3	0.21%
89	0.86	13.1	0.20%
83	1.53	25.7	0.20%
81	1.29	35.0	0.20%
70	1.01	10.3	0.20%
88	1.45	37.3	0.20%
15	1.80	45.8	0.20%
84	1.54	32.9	0.19%
187	1.69	38.8	0.19%
177	2.31	41.7	0.19%
123	2.92	32.3	0.19%
192	1.60	30.8	0.18%
194	1.38	22.0	0.18%
57	2.33	35.1	0.18%
7	4.07	83.5	0.18%
185	1.84	43.1	0.17%
49	1.03	19.9	0.17%
193	1.26	25.2	0.17%
178	2.24	37.3	0.17%
120	0.99	13.7	0.17%
12	2.89	45.4	0.17%
168	5.37	131.3	0.16%

80	2.30	21.2	0.16%
107	1.21	24.1	0.15%
98	1.80	39.0	0.15%
9	4.42	80.2	0.15%
72	0.88	21.4	0.15%
47	1.30	23.2	0.15%
78	1.84	38.8	0.15%
170	3.64	67.4	0.15%
20	1.51	26.6	0.15%
118	0.87	20.2	0.14%
42	1.47	35.6	0.14%
145	2.02	26.7	0.14%
56	1.00	9.1	0.14%
138	2.26	26.9	0.14%
55	0.89	22.1	0.14%
65	1.49	27.4	0.14%
121	1.34	36.7	0.14%
44	1.21	23.5	0.13%
16	1.50	36.1	0.13%
11	3.23	54.7	0.13%
156	4.24	70.3	0.13%
147	0.94	11.4	0.13%
140	0.88	23.0	0.13%
60	2.09	28.4	0.13%
26	0.74	12.6	0.13%
94	1.25	40.1	0.13%
93	1.81	37.8	0.12%
128	1.26	30.1	0.11%
181	2.69	37.4	0.11%
63	1.17	40.4	0.11%
45	0.83	13.0	0.11%
23	1.48	29.3	0.11%
129	1.81	31.1	0.11%
73	1.93	32.9	0.11%
58	2.04	37.5	0.11%
103	1.38	36.8	0.11%
126	1.26	26.2	0.11%
162	5.05	123.9	0.11%
39	1.68	26.1	0.11%
111	1.38	28.4	0.11%
77	1.00	17.2	0.10%
76	1.33	21.3	0.10%
134	1.27	33.9	0.10%
92	1.78	38.1	0.10%

40	1.02	11.3	0.10%
191	1.74	31.0	0.10%
32	1.05	11.3	0.10%
38	1.34	35.1	0.10%
41	1.44	26.7	0.10%
79	1.26	29.1	0.10%
6	4.21	69.4	0.10%
196	0.91	12.2	0.10%
108	0.93	13.3	0.10%
33	0.81	19.7	0.10%
85	1.14	22.4	0.10%
53	2.09	27.5	0.10%
52	1.54	30.8	0.09%
132	1.31	27.0	0.09%
135	1.38	29.5	0.09%
31	1.19	28.8	0.09%
127	1.79	32.0	0.08%
117	1.31	28.3	0.08%
64	1.30	38.3	0.08%
28	1.21	25.2	0.08%
190	2.03	25.8	0.08%
109	1.46	30.7	0.08%
43	1.25	32.9	0.08%
143	0.91	14.5	0.08%
59	1.30	21.7	0.08%
22	1.53	35.5	0.07%
27	1.10	25.3	0.07%
179	2.39	38.1	0.07%
155	4.17	71.7	0.07%
142	0.86	11.2	0.07%
195	1.04	13.1	0.07%
90	2.04	28.2	0.07%
139	2.21	19.5	0.06%
74	1.74	27.5	0.06%
164	5.44	136.0	0.06%
167	5.36	130.1	0.06%
114	1.24	22.0	0.06%
34	2.47	36.6	0.06%
112	1.60	26.1	0.06%
131	1.84	32.0	0.05%
110	1.01	8.1	0.05%
119	1.20	36.9	0.05%
25	2.41	37.3	0.05%
62	1.31	25.2	0.05%

48	1.19	30.5	0.05%
91	1.29	33.1	0.05%
97	1.16	36.4	0.05%
130	1.30	24.2	0.05%
82	0.95	9.0	0.04%
137	2.16	35.8	0.04%
149	0.84	12.2	0.03%
171	3.46	72.6	0.03%
29	1.03	21.5	0.03%
189	2.40	32.3	0.03%
172	4.27	60.5	0.03%
87	0.89	10.3	0.03%
10	3.13	47.5	0.03%
24	1.26	32.0	0.03%
174	2.47	42.9	0.03%
150	1.30	30.8	0.02%
18	0.81	10.3	0.02%
54	1.38	35.6	0.02%
75	1.73	38.2	0.02%
101	1.54	28.4	0.01%
51	1.32	22.3	0.01%
99	2.28	35.0	0.01%

[1] Green shading denotes the top four peaks observed in the pure gracilioether L spectrum (Table S9). These peaks were identified after the pure material was obtained to emphasize that many of the high scoring peaks in the mixture came from a single compound, namely gracilioether L (Table S9).

[2] Peak is a number that identifies the order that the peaks were abstracted from the raw data.

Table S9. Atomic novelty scores for gracilioether L

peak[1]	position[2]	δ_H	δ_C	distance
16	11	6.63	154.9	3.51%
1	5	6.47	142.1	1.00%
21	18	0.77	8.2	0.94%
3	21	3.65	51.1	0.75%
18	16	1.16	12.2	0.47%
2	2	4.85	84.0	0.40%
9	10	2.07	45.9	0.36%
4	9α	1.46	35.2	0.31%
14	8α	1.18	22.4	0.22%
12	14	2.24	26.9	0.18%
10	17β	1.78	32.0	0.17%
20	15	2.20	19.5	0.17%
19	9β	1.31	35.2	0.16%
5	19α	1.50	28.3	0.14%
6	7β	1.73	38.5	0.14%
15	8β	1.15	22.4	0.14%
11	20	0.85	12.0	0.13%
17	12	6.02	132.2	0.09%
13	19β	1.35	28.3	0.09%
8	17α	1.85	32.0	0.08%
7	7α	1.83	38.5	0.04%

[1] Peak is a number that identifies the order that the peaks were abstracted from the raw data.

[2] Position identifies the atom number based on those given in Ueoka, R.; Nakao, Y.; Kawatsu, S.; Yaegashi, J.; Matsumoto, Y.; Matsunaga, S.; Furihata, K.; van Soest, R. W. M.; Fuestani, N. *J. Org. Chem.* **2009**, *74*, 4203-4207.

Table S10. NMR spectral data for gracilioether L in CD_3OD

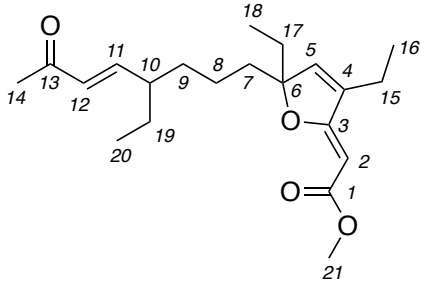

gracilioether L

Position	δ_C, Type	δ_H, mult (*J* in Hz)	^1H-^1H COSY	^1H-^{13}C HMBC
1	169.3, C	-		
2	84.0,CH	4.85, s	5w	3,4
3	174.2,C	-		
4	141.4,C	-		
5	142.1,CH	6.47, t (1.7)	2w,15	1w,3,4,6,15
6	99.7,C	-		
7α	38.5,CH_2	1.83, m	7β,8β	5w,6w,8,9,17
7β		1.73, m	7α,8α	5w,6w,8,9,17w
8α	22.4,CH_2	1.18, m	7α,7β,8β,9β	6,7,9,10
8β		1.15, m	7α,7β,8α,9α	6,7,9,10
9α	35.2,CH_2	1.46, m	8β,10	7,8,10,11,19w
9β		1.31, m	8α,10	7,8,10,11,19w
10	45.9,CH	2.07, m	9α,9β,11,19α,19β	8,9,11,12,19,20
11	154.9,CH	6.63, dd (16.0, 9.2)	10,12	9,10,13,19
12	132.2,CH	6.02, d (0.8, 16.0)	11,14w	9w,10,13,14,19w
13	201.3,C	-		
14	26.9,CH_3	2.24, s	11w	11,12,13
15	19.5,CH_2	2.20, qt (7.4,1.7)	5,16	3,4,5,16
16	12.2,CH_3	1.16, t (7.4)	15	4,15
17α	32.0,CH_2	1.85, m	18	5,6,7,18
17β		1.78, q (7.2)	18	5,6,7w,18
18	8.2,CH_3	0.77, t (7.4)	17α,17β	6,17
19α	28.3,CH_2	1.50, m	10,19β,20	9,10,11,20
19β		1.35, m	10,19α,20	9,10,11,20
20	12.0,CH_3	0.85, t (7.5)	19α,19β	10,19
21	51.1,CH_3	3.65, s		1

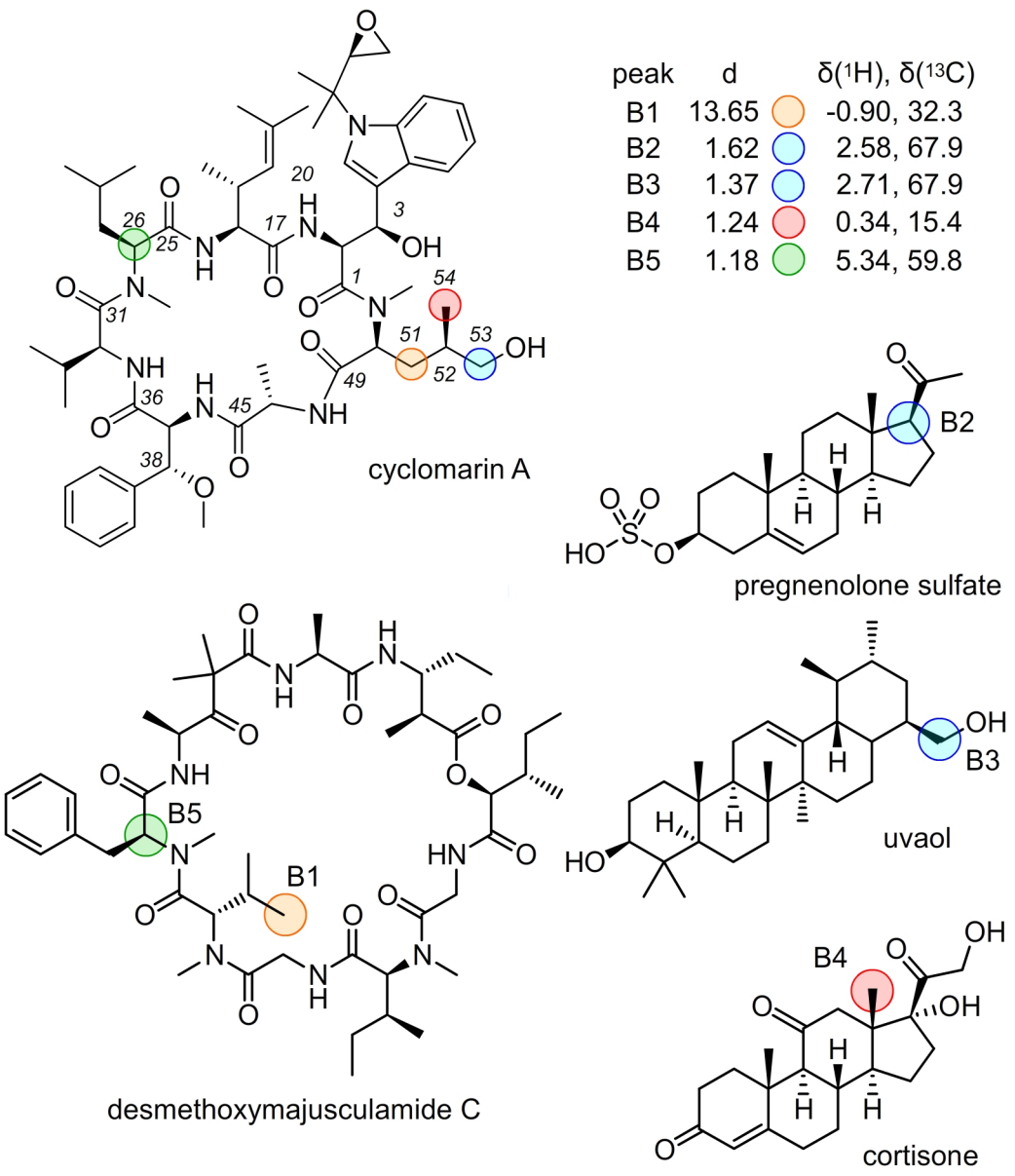

Figure S1. Peak comparative analyses for cyclomarin A. The structures producing the top prioritized peaks in cyclomarin A are compared with the compounds producing their closest peak within the database as shown in Fig. 2 of the manuscript. The closest peak to B1 was from a side chain methyl of an *N*-methylvaline residue in desmethoxymajusculamide C. Interestingly, both the methyl in desmethoxymajusculamide C and methylene within cyclomarin A were directly proximal to an *N*-methylated amide and shared a comparable environment. The second and third peaks B2 and B3 were close to peaks in pregnenolone sulfate and uvaol, respectively. While the former was not a good fit, the later demonstrated a very similar chemical shift environment with the C53 in cyclomarin A sharing a common motif (blue circle) with uvaol. Peaks B4 and B5 showed also similar correlations with methyl groups (cyclomarin A *versus* cortisone) and α-protons on an amino acid within a cyclic peptide or despipeptide. Remarkably, this small database was able to return structures for each peak with a reliable counterpart.

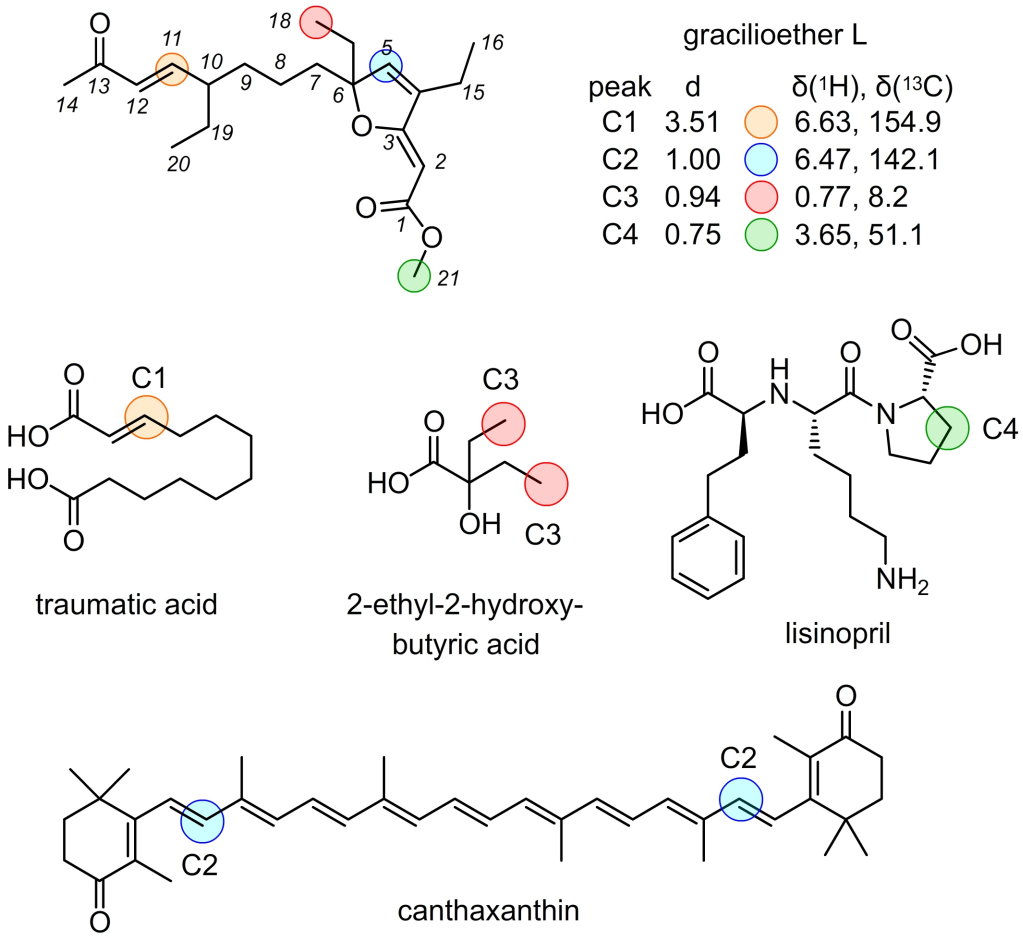

Figure S2. Peak comparative analyses for gracilioether L. The closest peak in the database to C1 was the β-position of traumatic acid, a functionality that directly correlated with the β-position of the *trans*-enone in gracilioether L. Peak C2 again shared remarkable similarity to its most proximal peak. Here, C2, a δ proton within an unconjugated ester, was proximal to an olefin peak that correlated to δ proton of an unsaturated ketone within canthaxanthin. The closest peak to C3 also contained a high degree of similarity being contained within an ethyl group proximal to hydrogen bond donating oxygen atom and a carbonyl. Peak C4 did not show comparable peaks due to a lack of methyl esters in our database. The latter point suggests the needs to develop an intelligent database, one that offers clear predictions for each peak and enables one to generate structural assignments. Eventually, this would need to be paired with correlation data from 2-bond and 3-bond couplings from spectra such as ^{1}H-^{13}C HMBC spectra to automate *de novo* structural assignment.

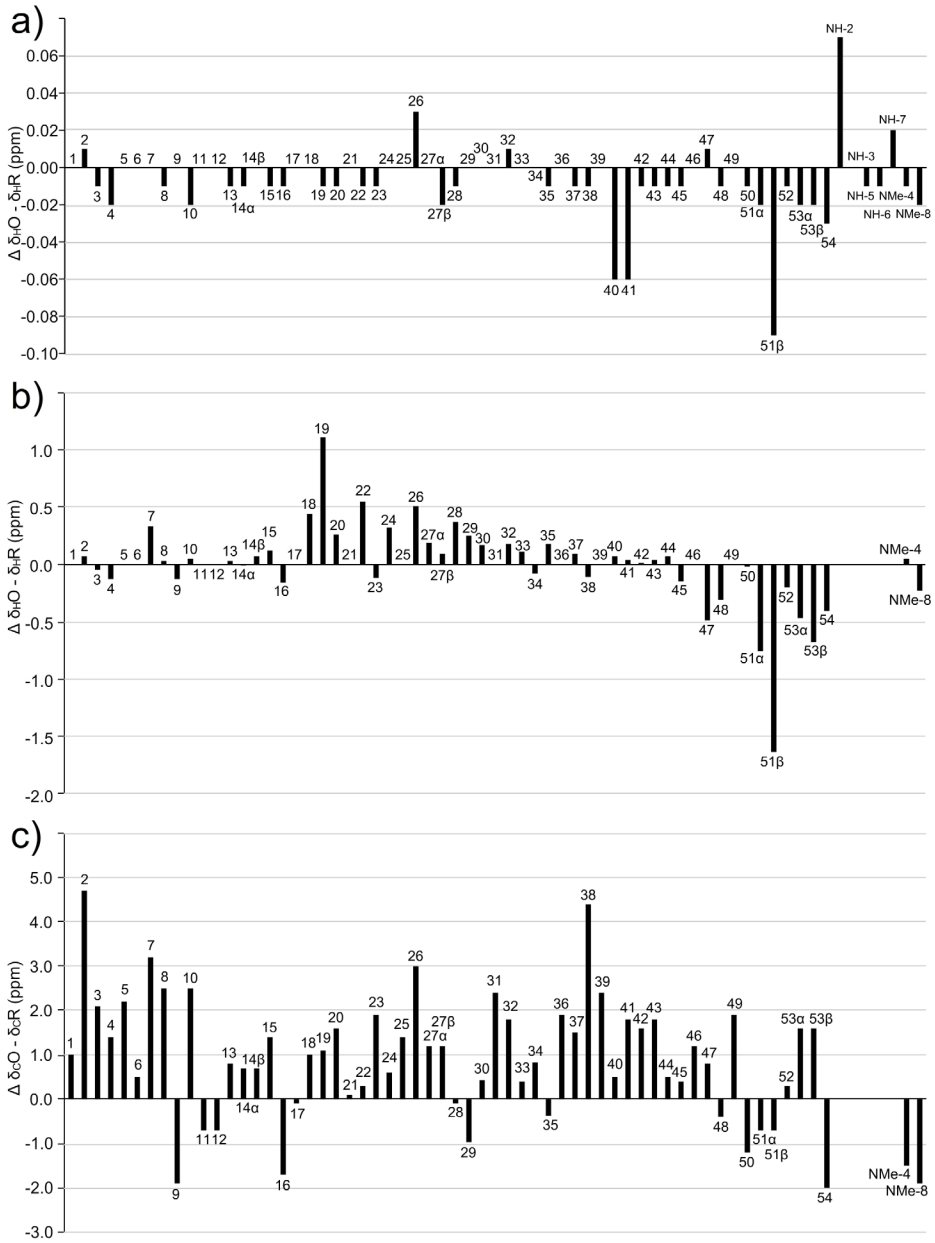

Figure S3. Peak shift analyses for cyclomarin A. Our NMR studies were conducted in CD_3OD while the reported characterization of isolated cyclomarin A [M. K. Renner, Y.-C- Shen, X.-C. Cheng, P. R. Jensen, W. Frankmoeller, C. A. Kauffman, W. Fenical, E. Lobkovsky, J. Clardy, *J. Am. Chem. Soc.* **1999**, *121*, 112736] (isolation data) and material produced *via* total synthesis [P. Barbie, U. Kazmaier, *Org. Lett*. **2016**, *18*, 204-7] was conducted in $CDCl_3$. As noted in these publications the chemical shifts and coupling constants of cyclomarin A modulate according to concentration and amounts of water present. **a)** Comparison of the proton chemical shifts from cyclomarin A isolated herein in $CDCl_3$ against the isolation data in $CDCl_3$. **b)** Comparison of the proton chemical shifts from cyclomarin A isolated herein in CD_3OD against the isolation data in $CDCl_3$. **c)** Comparison of the carbon chemical shifts from cyclomarin A isolated herein in CD_3OD against the isolation data in $CDCl_3$. Both proton in b) and carbon c) shift perturbations illustrate the complexities associated with the use of different solvents.

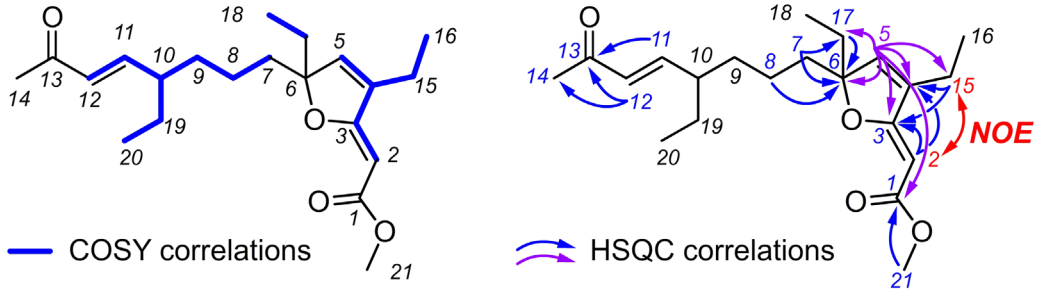

Figure S4. Structure elucidation of gracilioether L. Gracilioether L was isolated as a wax with molecular formula $C_{21}H_{32}O_4$ inferred by high resolution ESI HRMS (M+Na$^+$, *m/z* 371.2193 calcd. 371.2198). The ^{1}H-^{13}C HSQC indicated the presence of 3 ethyl groups, 3 contiguous methylenes, 1 acyl group, a carbomethoxyl, a sp^3 methine, an unusually high field sp^2 methine, a 1,2, disubstituted double bond, and a trisubstituted double bond. ^{1}H-^{1}H COSY correlations defined a spin system consisting of the disubstituted double bond (H11,H12), the methine (H10), one of the ethyl groups (H19,H20) and the three adjoining methylenes (H9,H8,H7). ^{1}H-^{13}C HMBC correlations placed the acetyl group (H14 and C13) to the other side of the disubstituted double bond (H12). ^{1}H-^{13}C HMBC correlations to the trisubstituted double bond (H5) identified three quaternary carbons (C3,C4,C6) that were also linked to the remaining two ethyl groups and the highly upfield sp^2 methine. A literature search for similar chemical shifts suggested the trisubstituted cyclic ether framework. Initially, we envisioned C2 (δ_C 84.0) as an oxygenated methine but subsequently found it to be a part of a conspicuous furanylidene motif. The unusual chemical shifts of this group have been remarked upon several times [R. J. Capon, S. Singh, A. Sadaquat, S. Subramaniam, *Aust. J. Chem.* **2005,** *58*, 18-20 or D. B. Stierle, D. J. Faulkner, *J. Org. Chem*., **1980**, *45*, 3396-3401]. HMBC correlations positioned the remaining ethyl groups on the five membered ring and located the methoxyl as part of a methyl ester attached to the Δ^2 trisubstituted double bond. The C11-C12 double bond was assigned the trans configuration based on the 16.0 Hz coupling between H11 and H12. NOEs from H2 to H15 and H16 defined the Z geometry about the C2-C3 double bond.

Note: The stereochemistry at C6 and C10 could not be determined by NMR methods and would likely require validation by chemical synthesis.

Figure S5. $^{1}H-^{13}C$ HSQC database

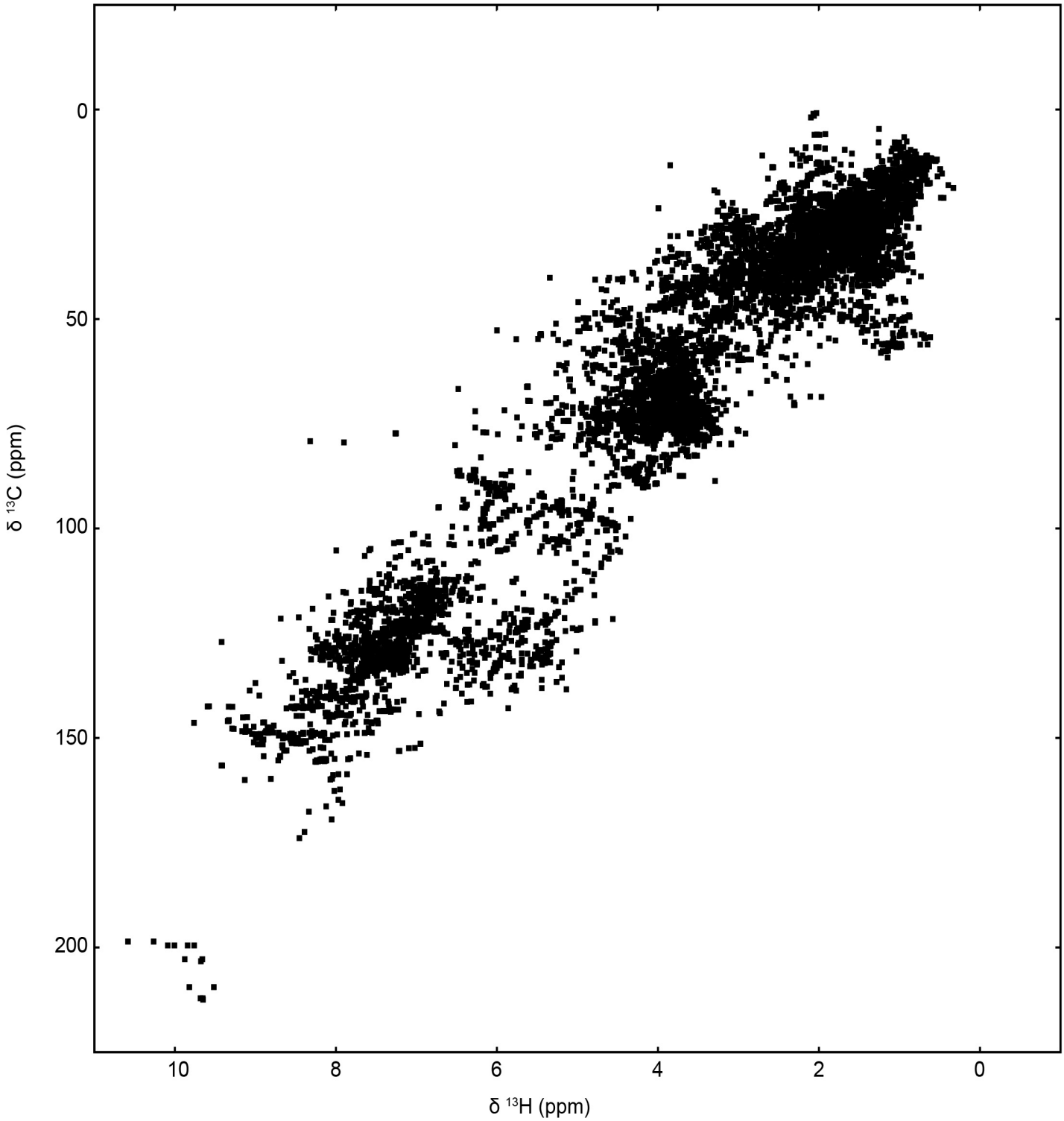

Figure S6. $^{1}H-^{13}C$ HSQC (600 MHz) spectrum of bromophycolide A in CD_3OD

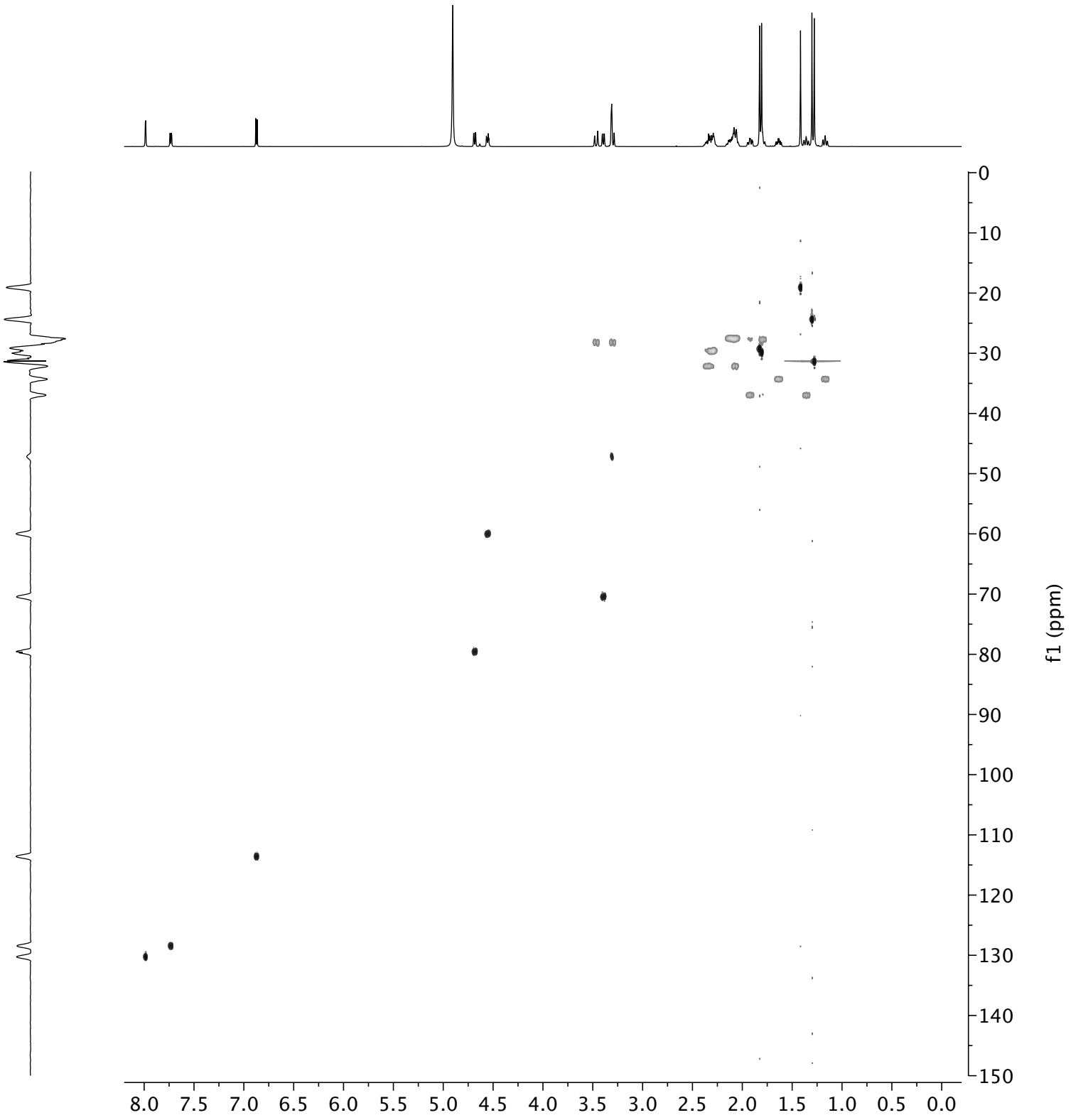

Figure S7. Profiled $^{1}H-^{13}C$ HSQC spectrum of bromophycolide A

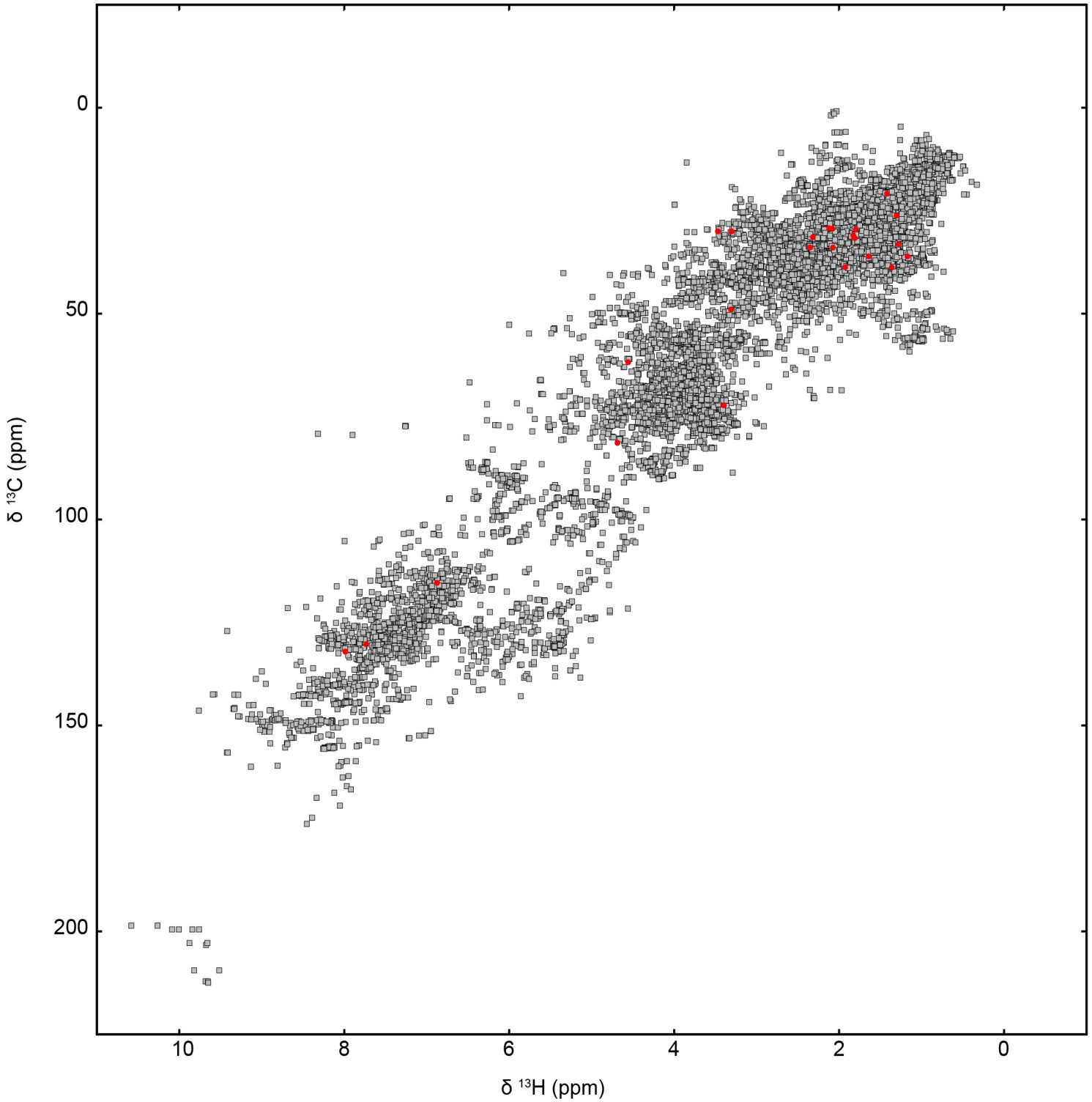

Figure S8. $^{1}H-^{13}C$ HSQC(600 MHz) spectrum of strychnine in CD_3OD

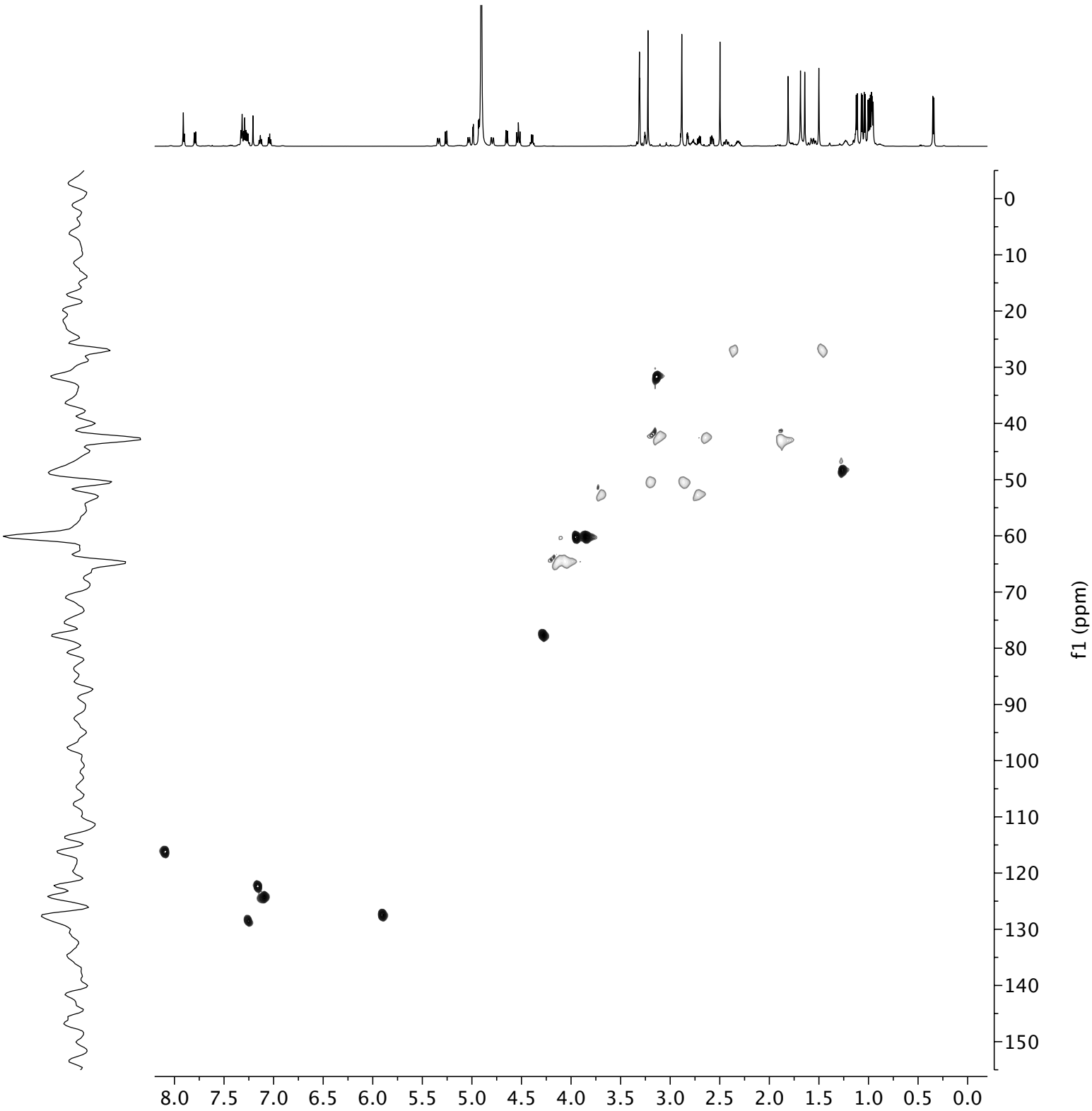

Figure S9. Profiled $^{1}H-^{13}C$ HSQC spectrum of strychnine

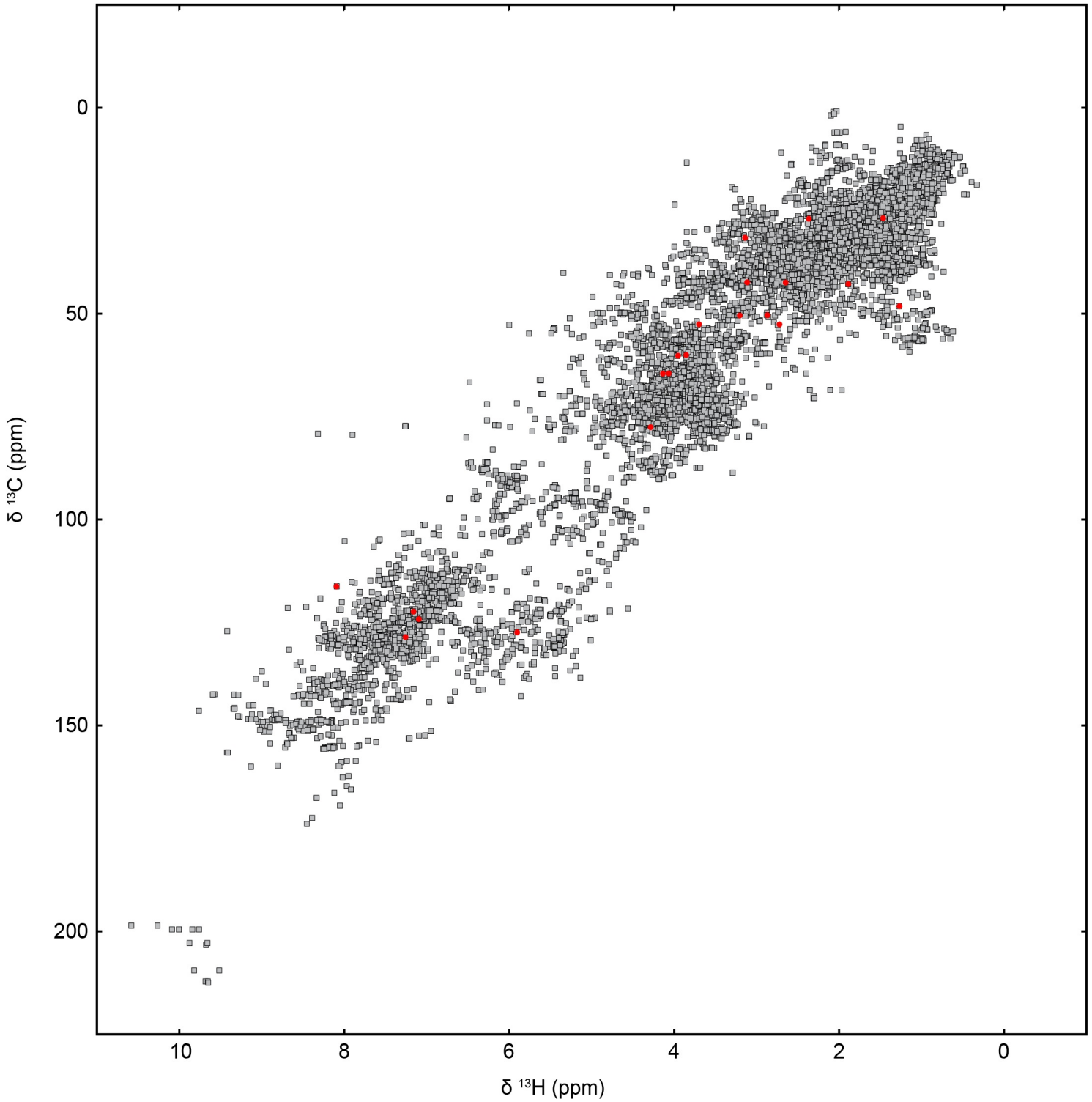

Figure S10. $^{1}H-^{13}C$ HSQC (600 MHz) spectrum of brusatol in CD_3OD

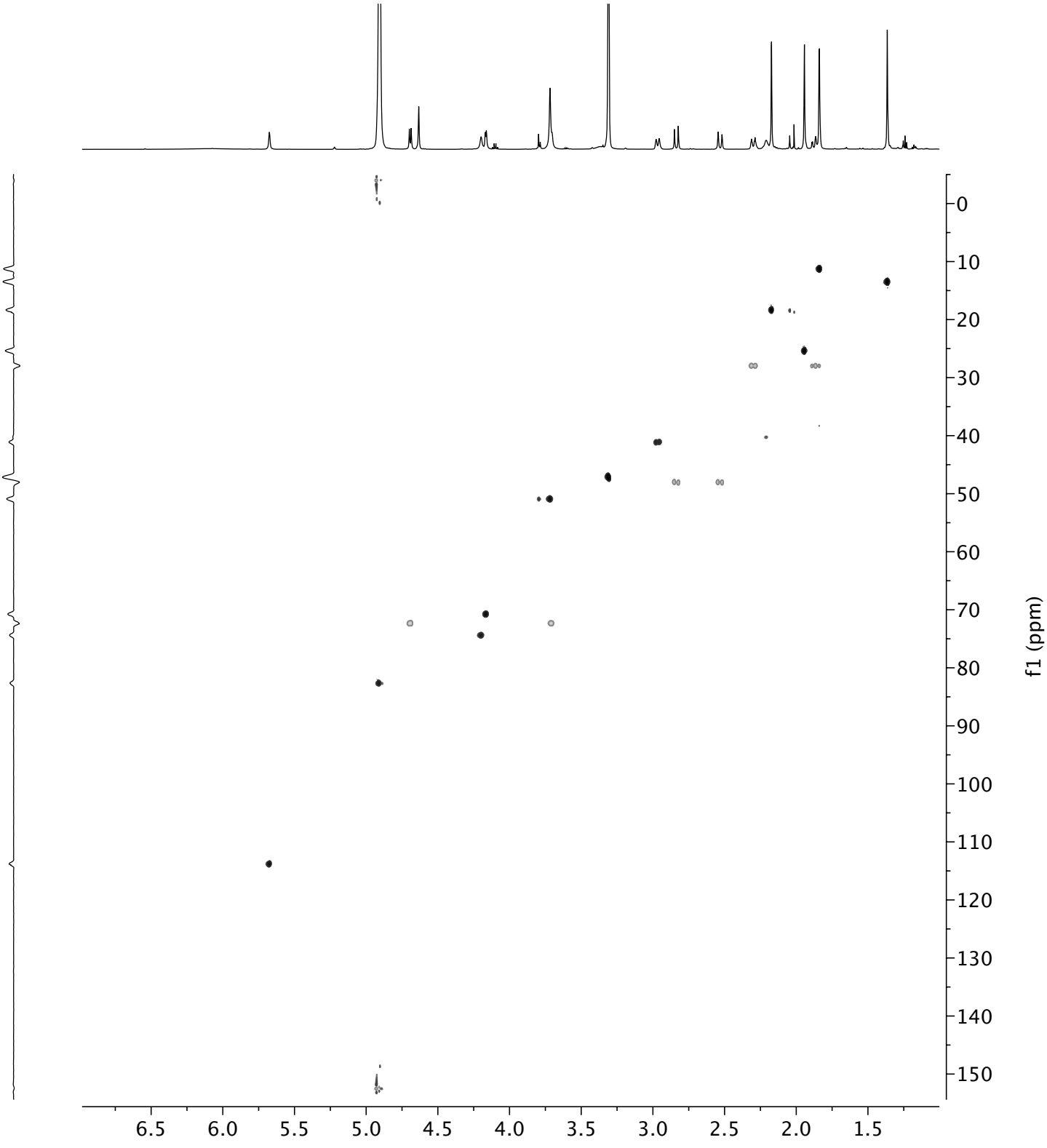

Figure S11. Profiled $^{1}H-^{13}C$ HSQC spectrum of brusatol

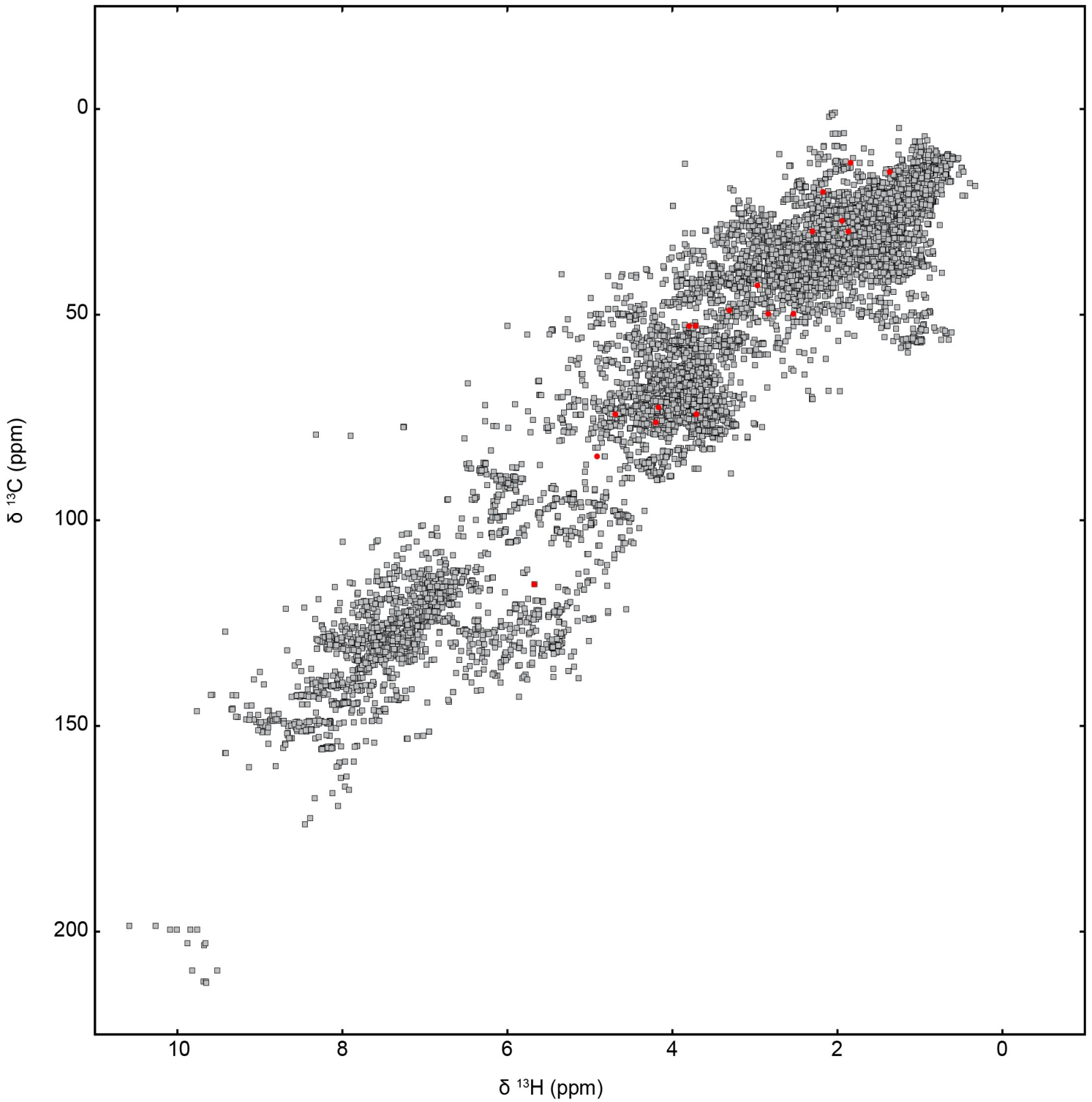

Figure S12. $^{1}H-^{13}C$ HSQC (600 MHz) spectrum of paclitaxel in CD_3OD

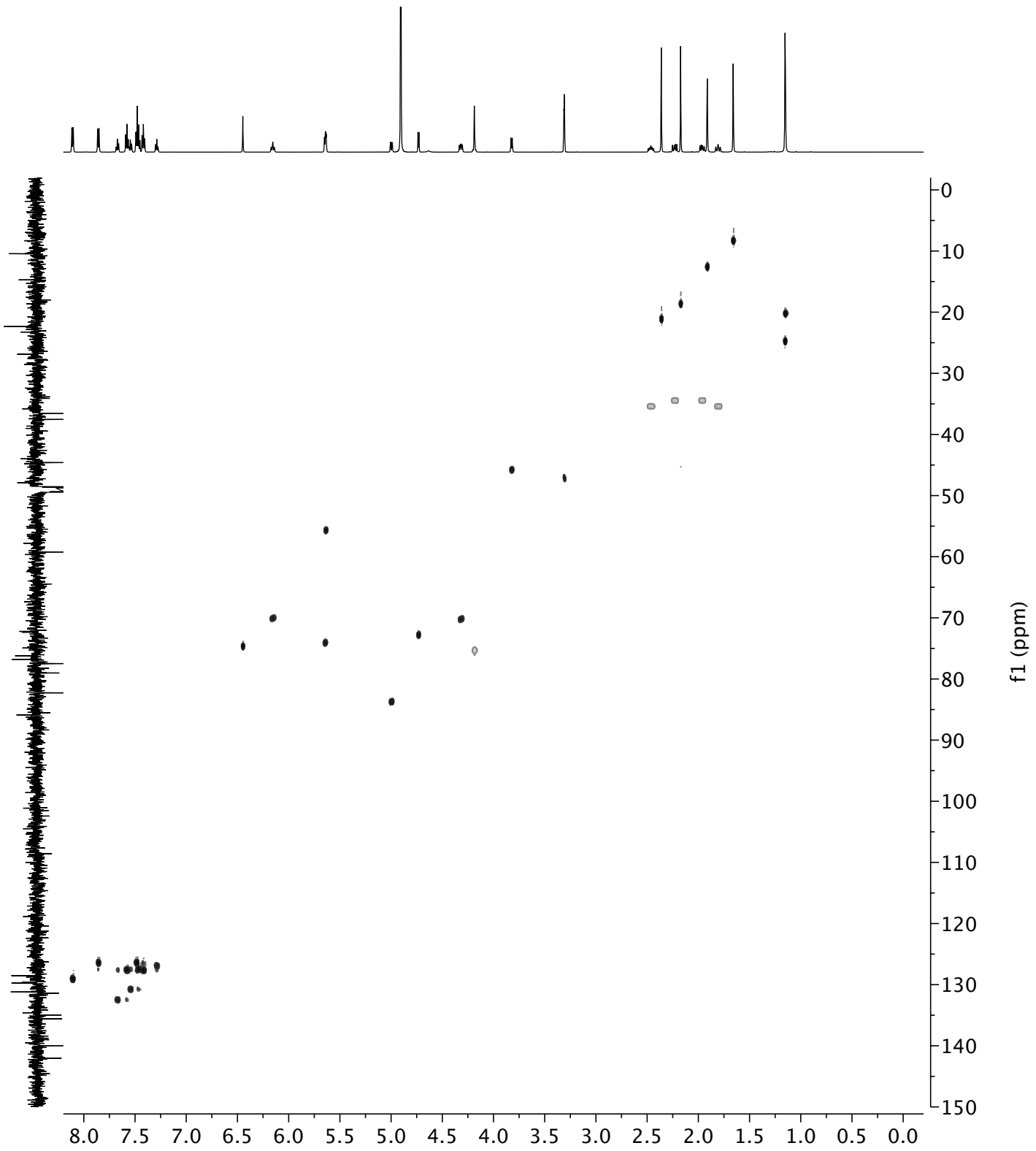

Figure S13. Profiled $^{1}H-^{13}C$ HSQC spectrum of paclitaxel

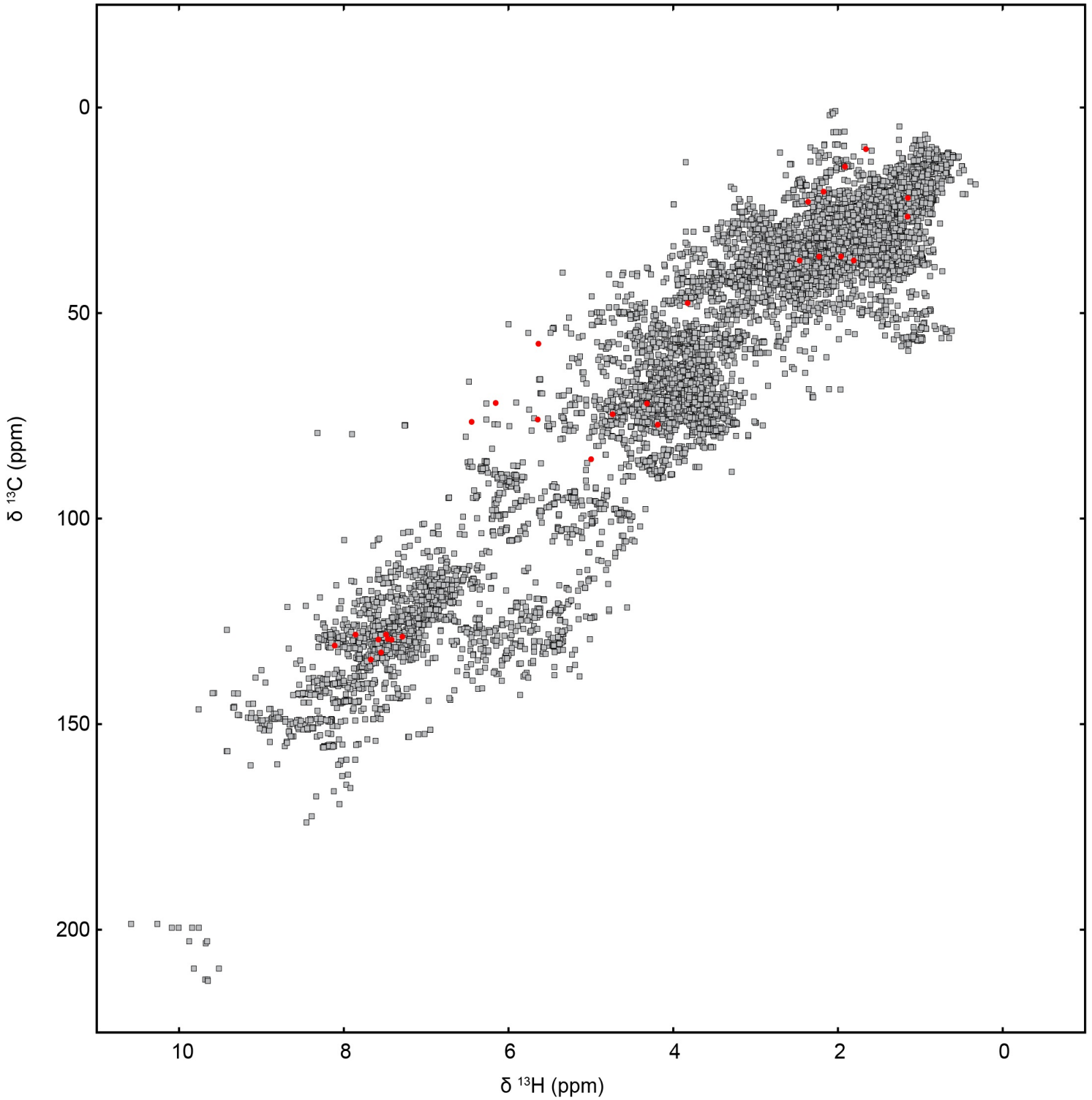

Figure S14. $^{1}H-^{13}C$ HSQC (600 MHz) spectrum of the CNB-982 extract in CD_3OD

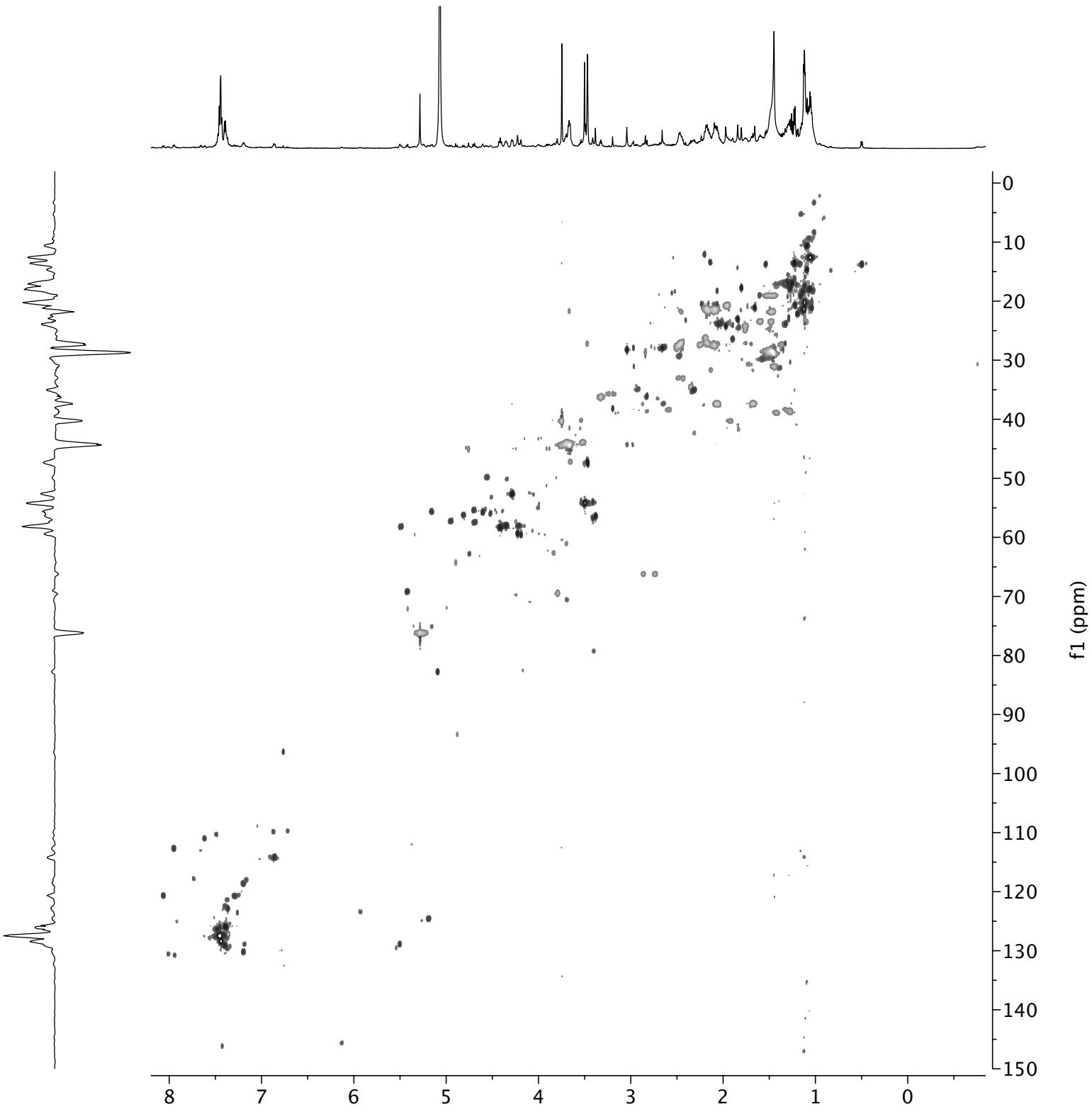

Figure S15. Profiled ^{1}H–^{13}C HSQC spectrum of the CNB-982 extract

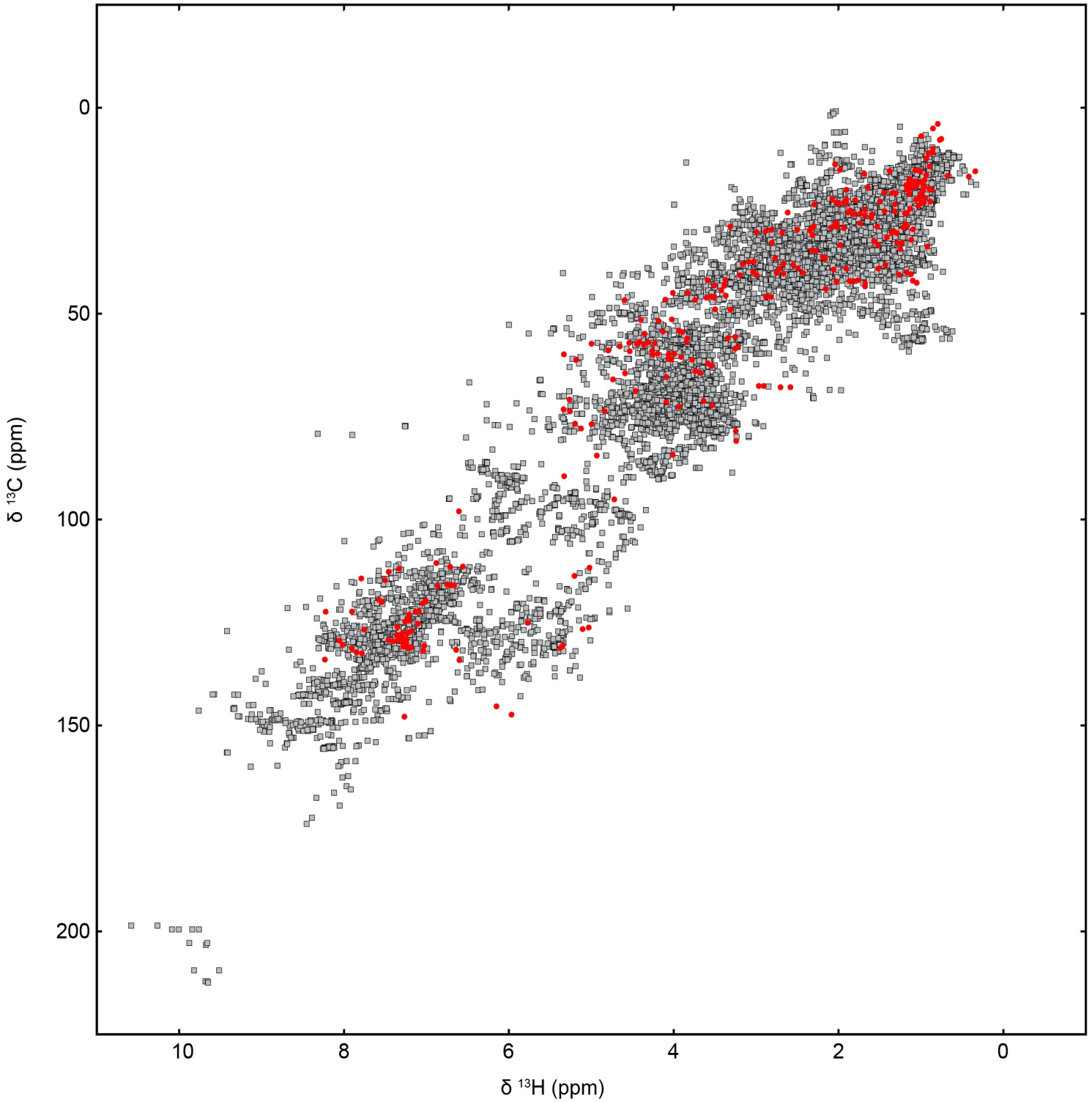

Figure S16. $^{1}H-^{13}C$ HSQC (600 MHz) spectrum of cyclomarin A in CD_3OD

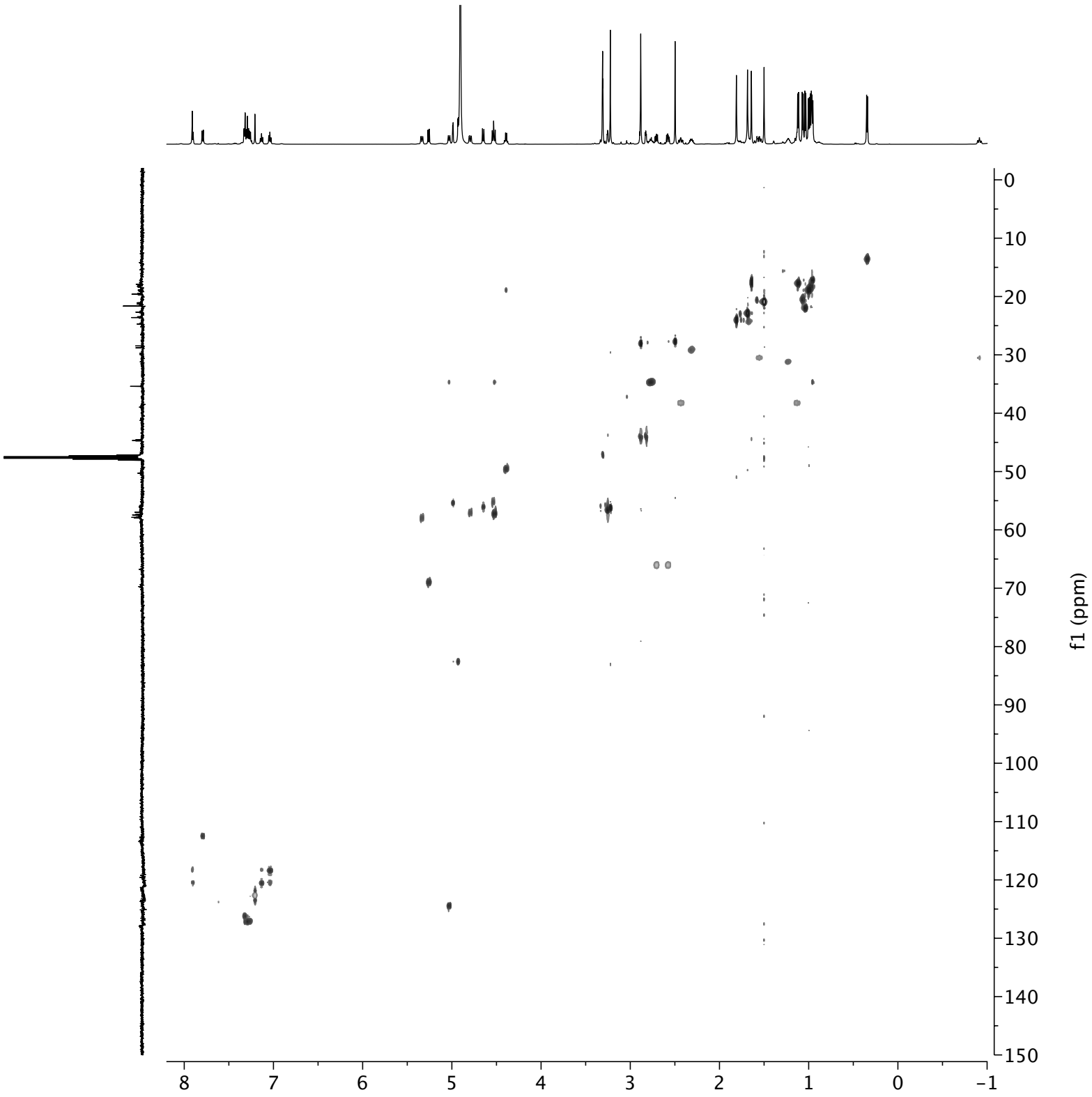

Figure S17. Profiled $^{1}H-^{13}C$ HSQC spectrum of cyclomarin A

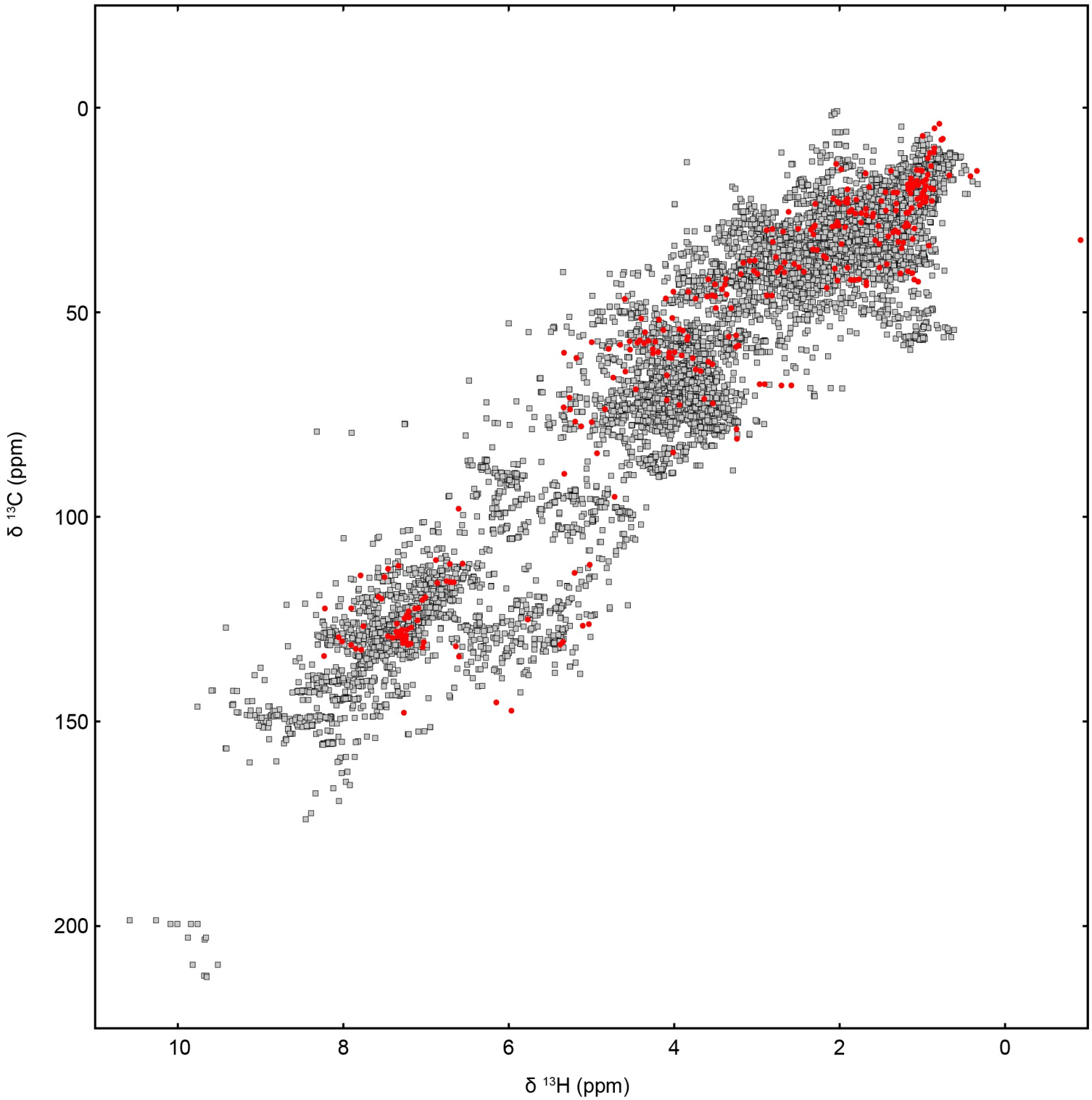

Figure S18. ^{1}H NMR (600 MHz) spectra of cyclomarin A in CD_3OD

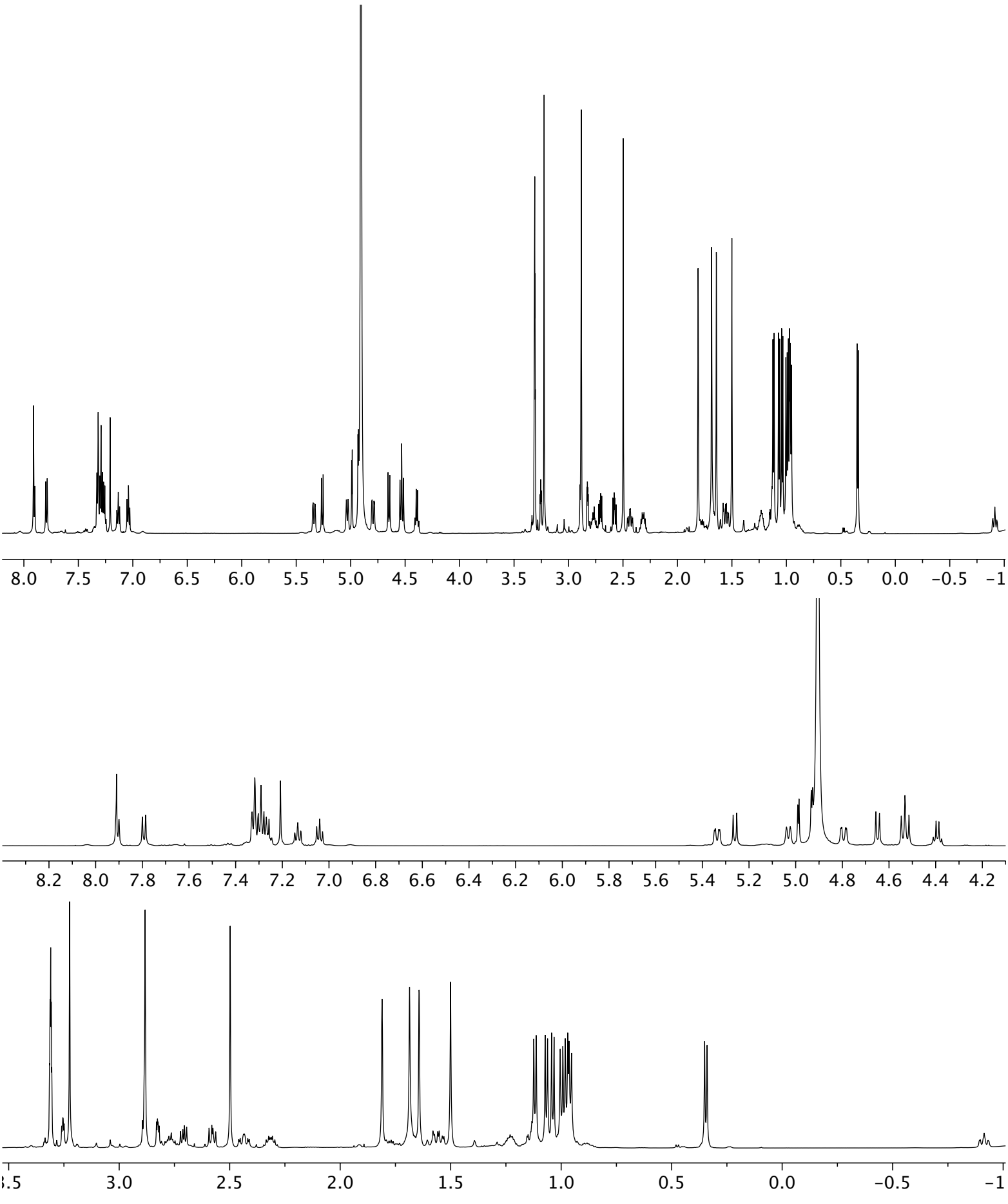

Figure S19. $^{1}H-^{1}H$ gCOSY (600 MHz) spectrum of cyclomarin A in CD_3OD

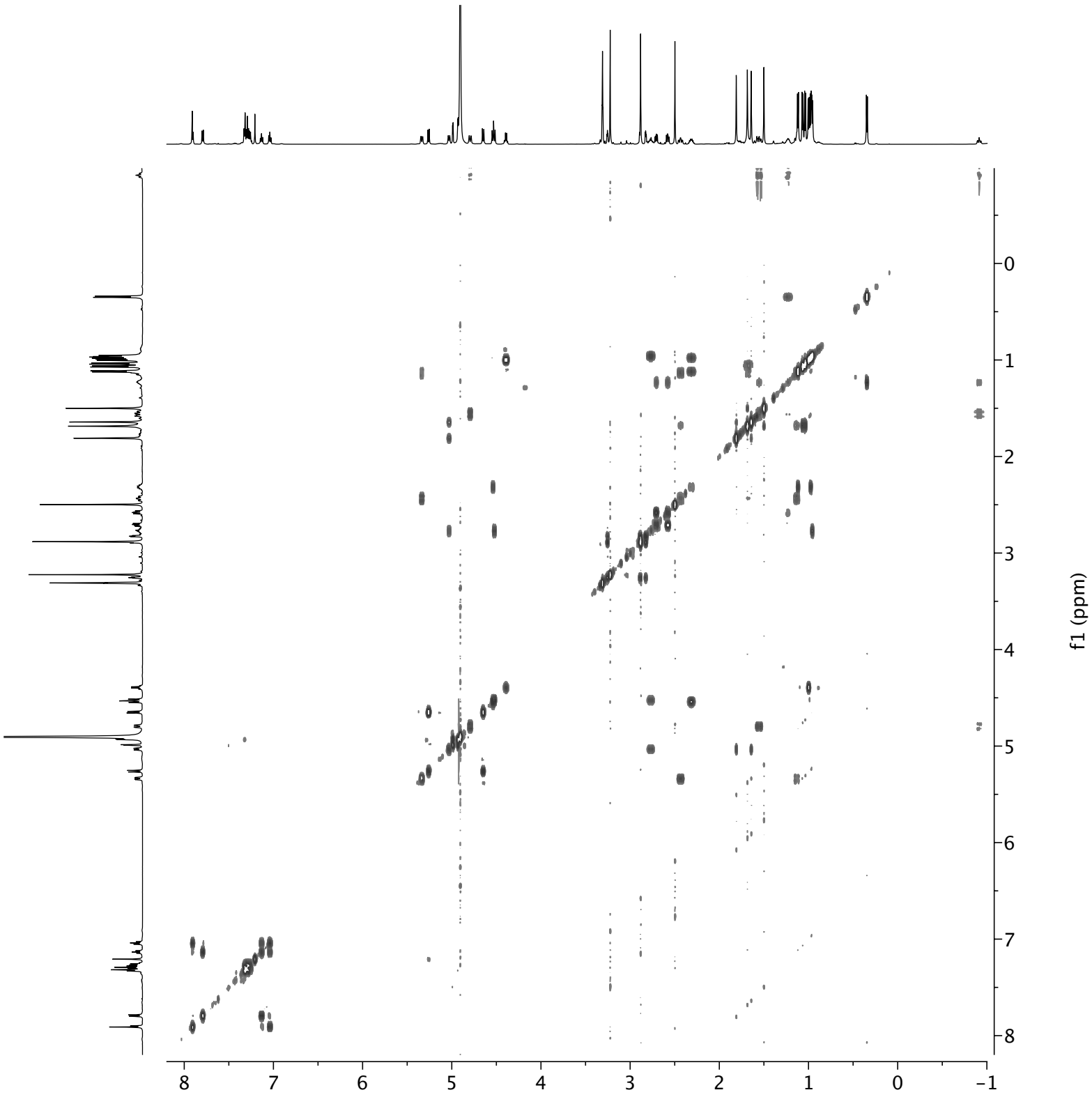

Figure S20. $^{1}H-^{13}C$ HMBC (600 MHz) spectrum of cyclomarin A in CD_3OD

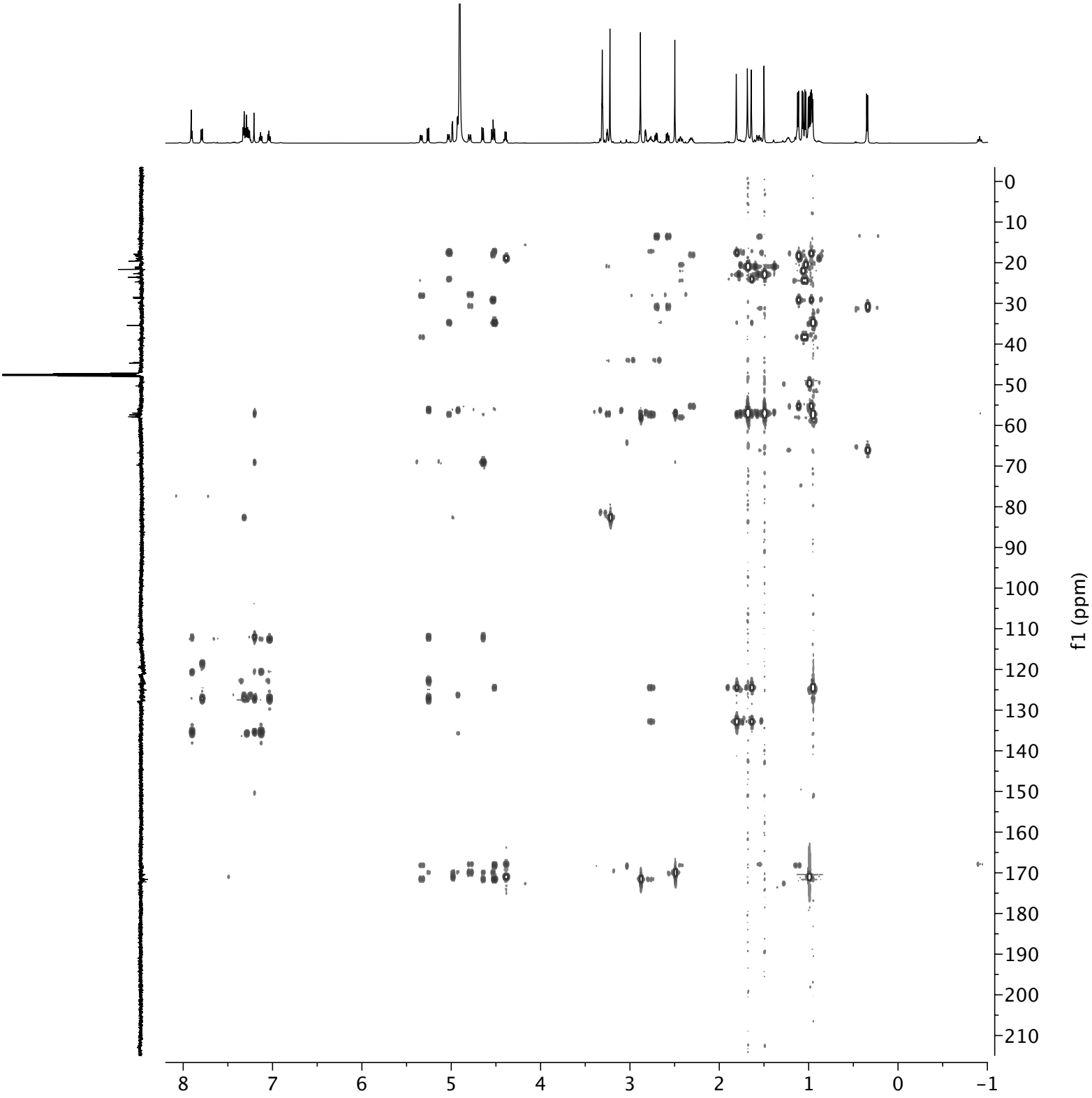

Figure S21. $^{1}H-^{13}C$ H2BC (600 MHz) spectrum of cyclomarin A in CD_3OD

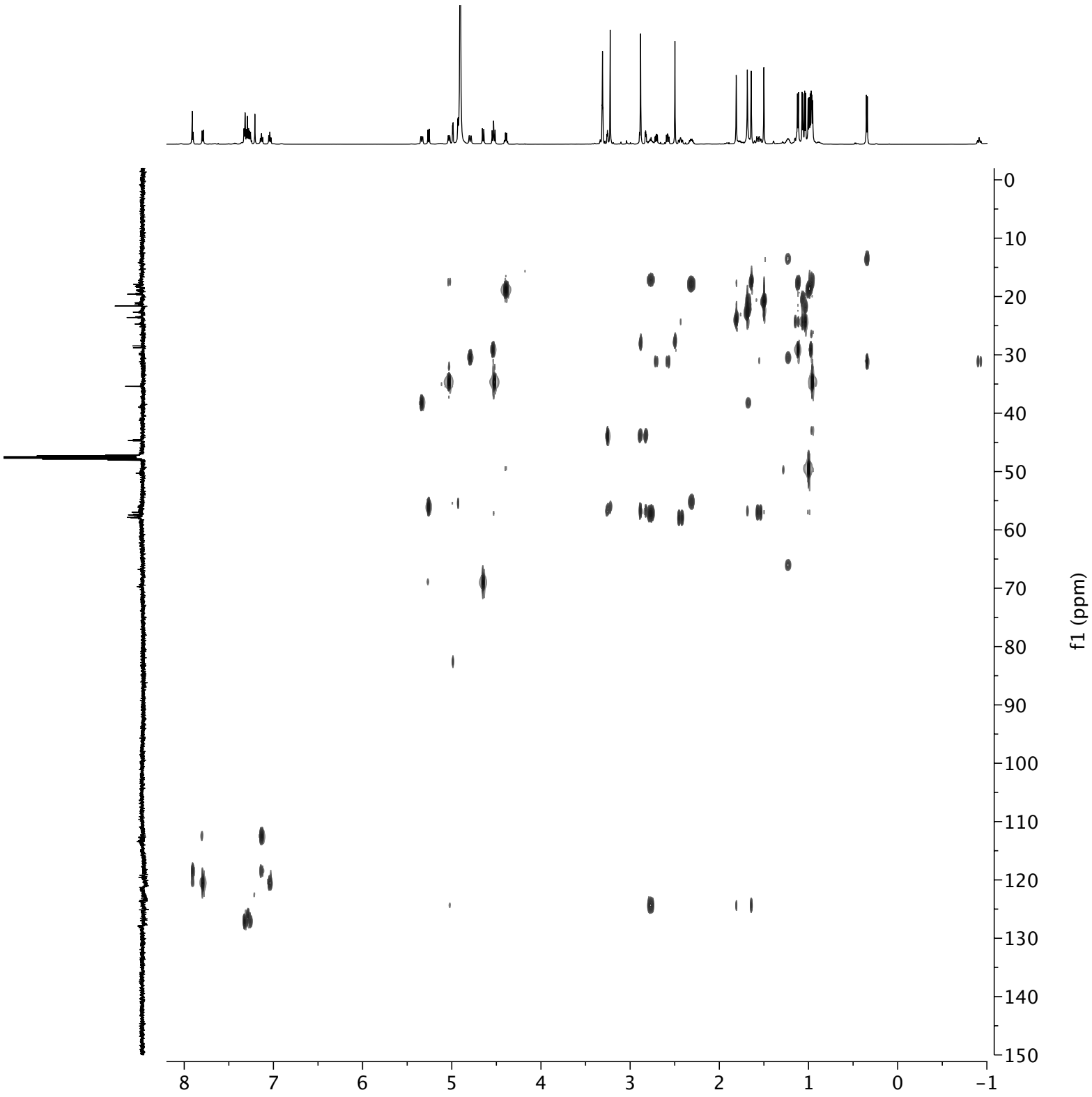

Figure S22. ^{1}H NMR (600 MHz) spectra of cyclomarin A in $CDCl_3$

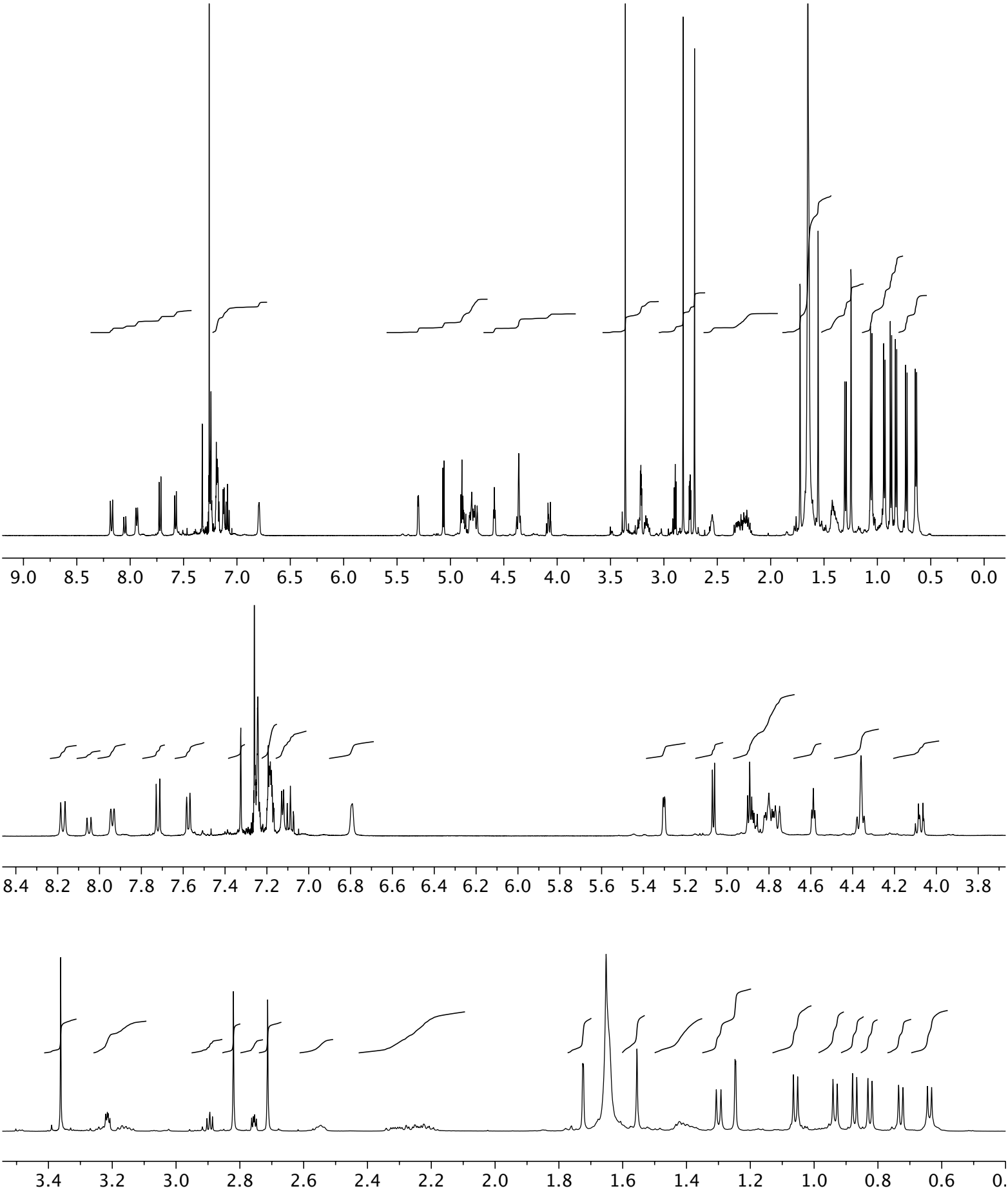

Figure S23. $^{1}H-^{13}C$ HSQC (600 MHz) spectrum of IM06-19 extract in CD_3OD

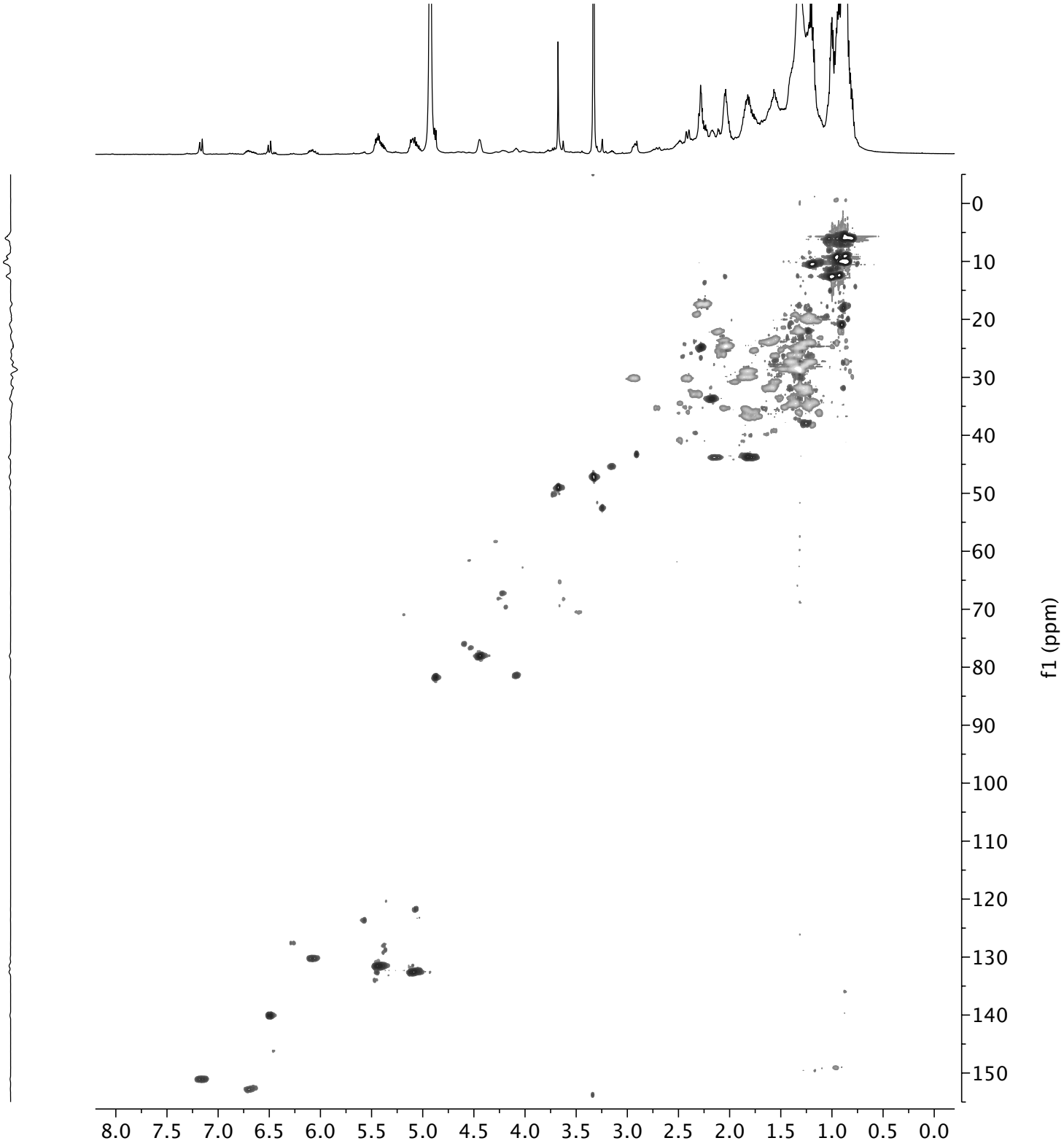

Figure S24. Profiled ^{1}H–^{13}C HSQC spectrum of the IM06–19 extract

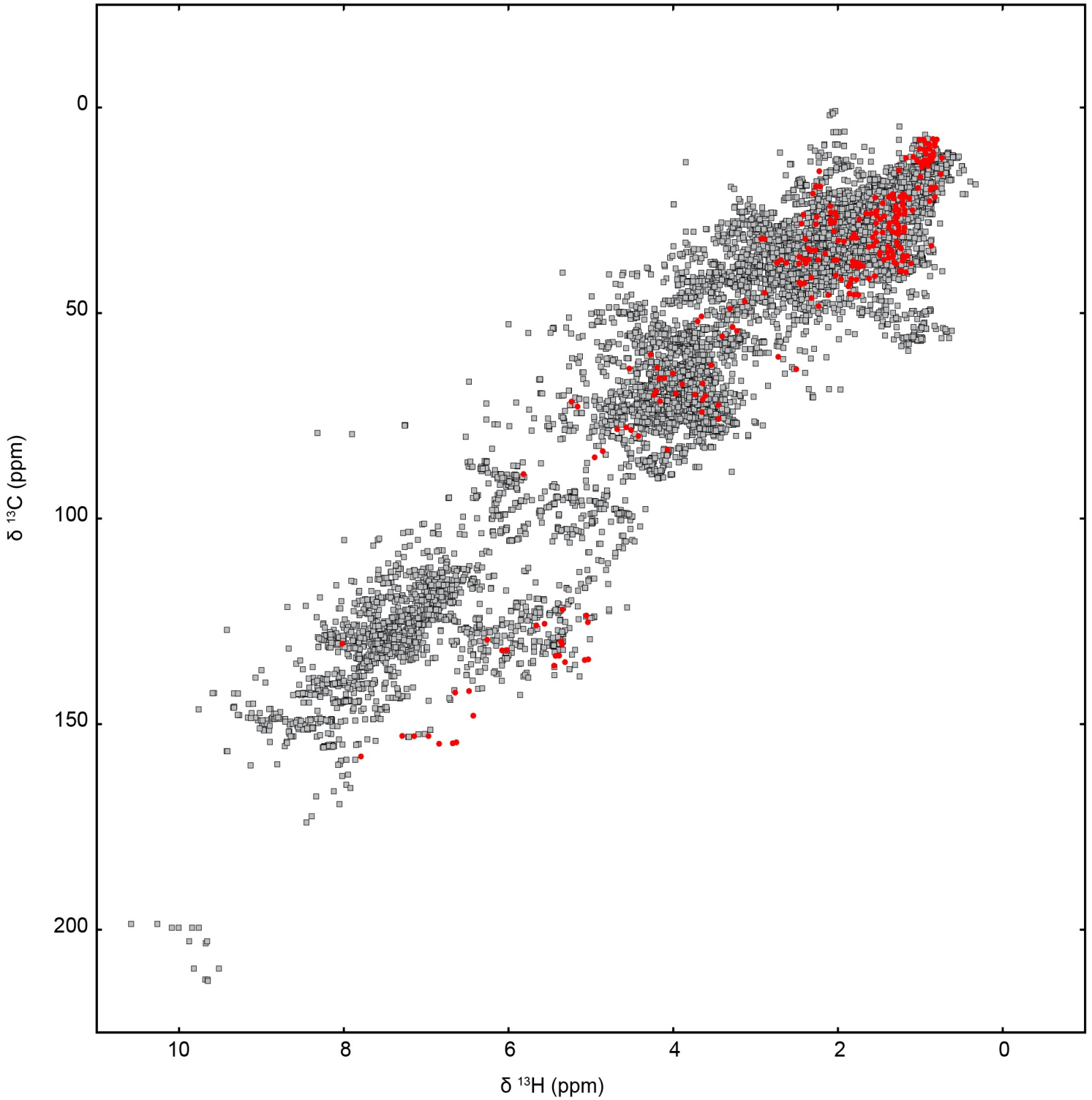

Figure S25. $^{1}H-^{13}C$ HSQC (600 MHz) spectrum of gracilioether L in CD_3OD

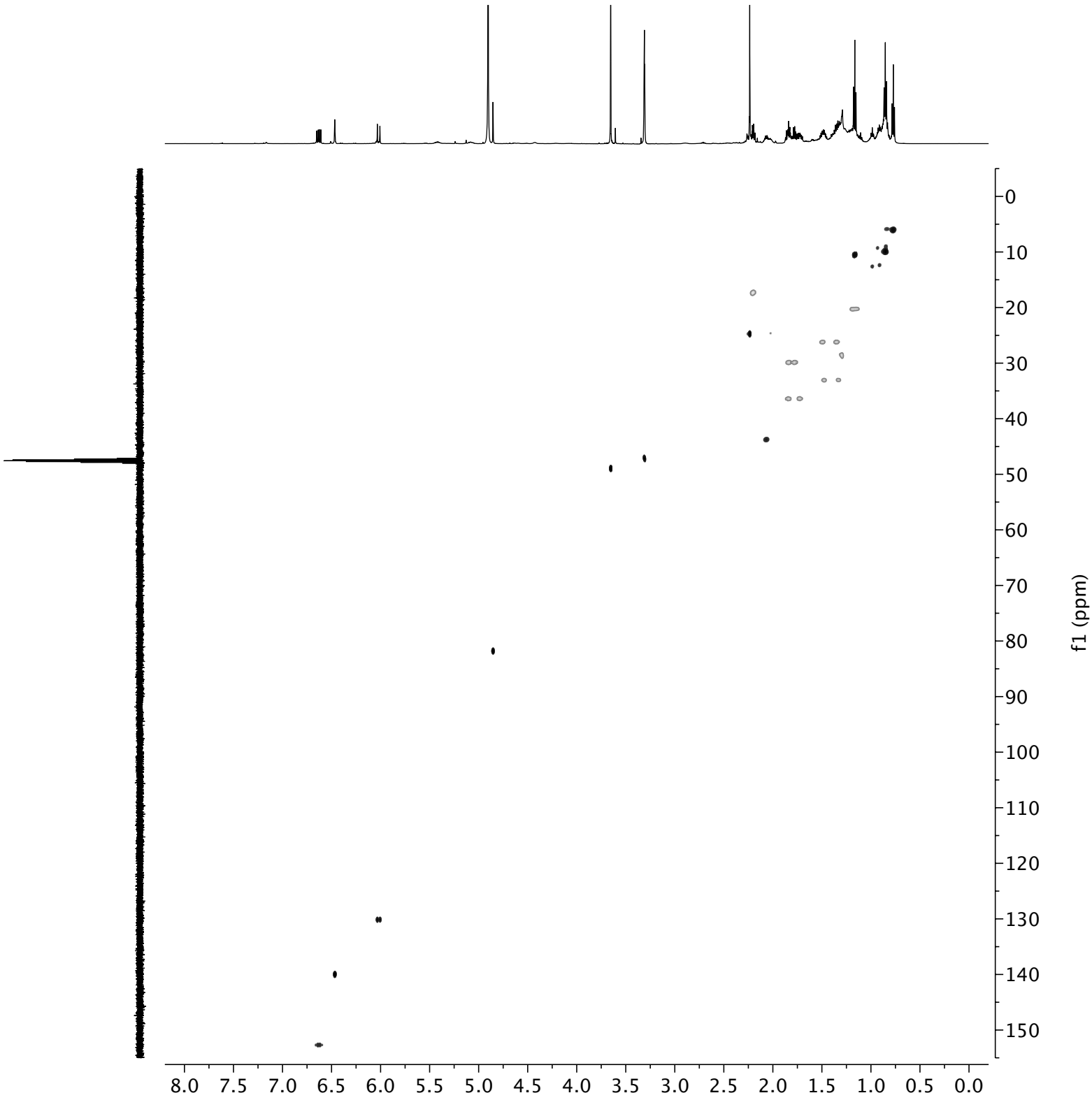

Figure S26. Profiled $^{1}H-^{13}C$ HSQC spectrum of of gracilioether L

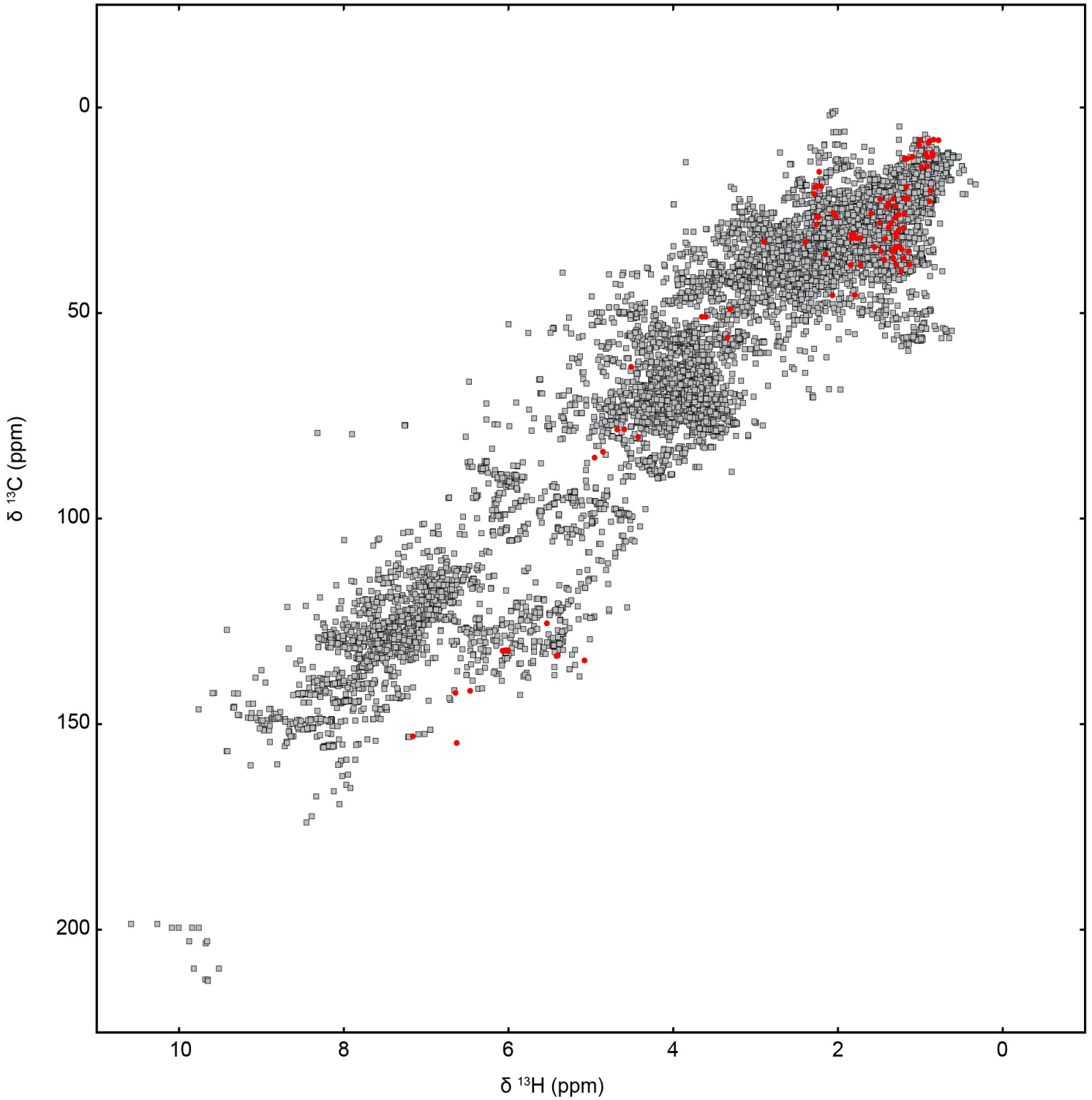

Figure S27. ^{1}H NMR (600 MHz) spectra of gracilioether L in CD_3OD

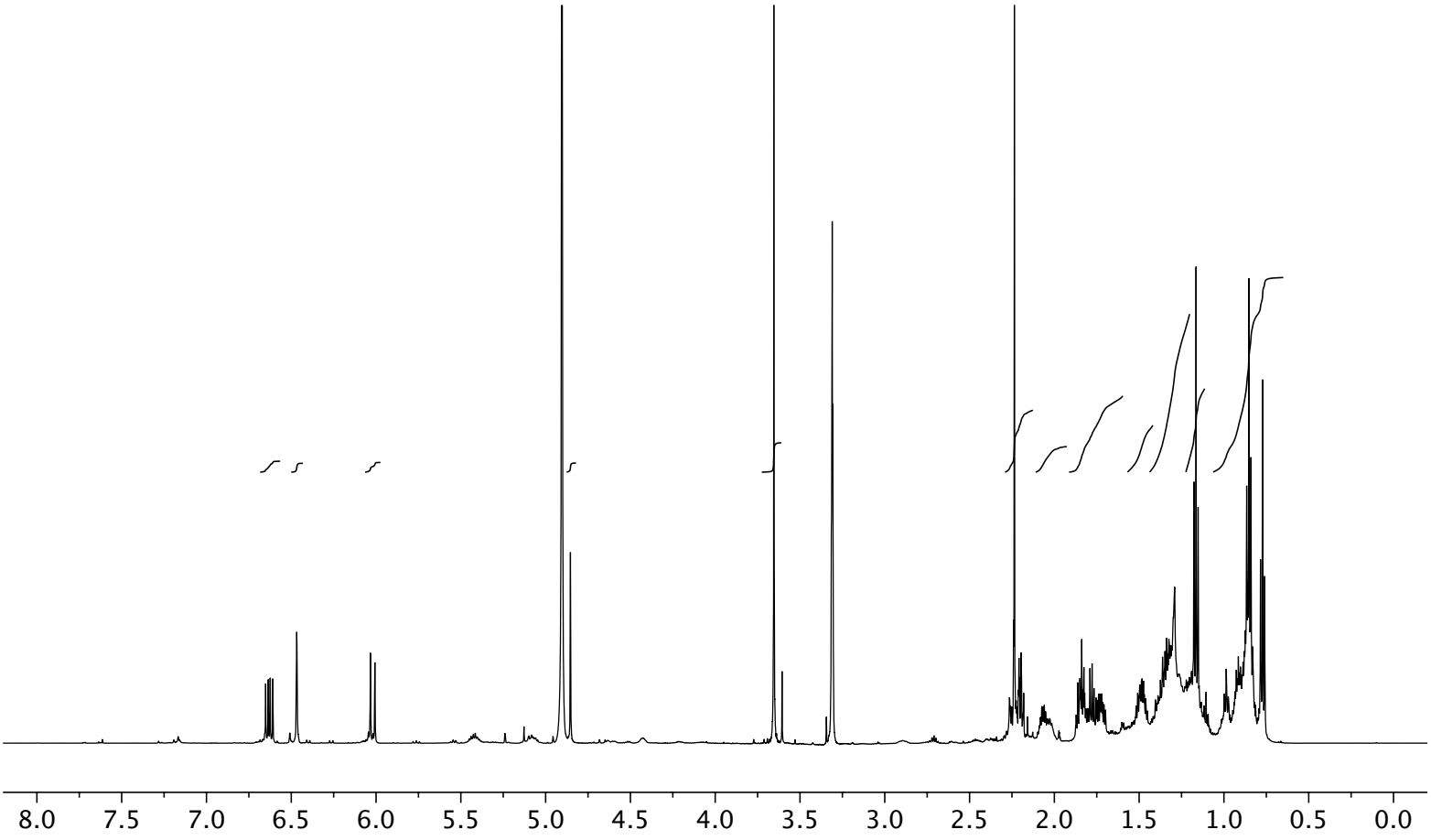

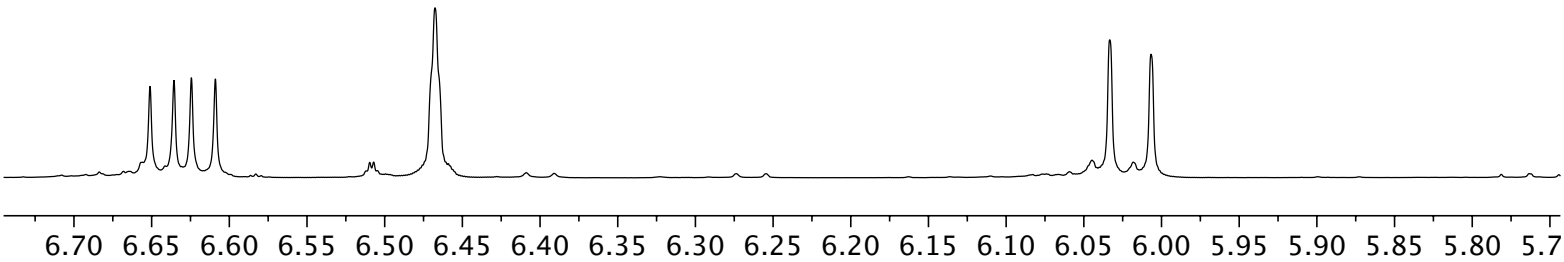

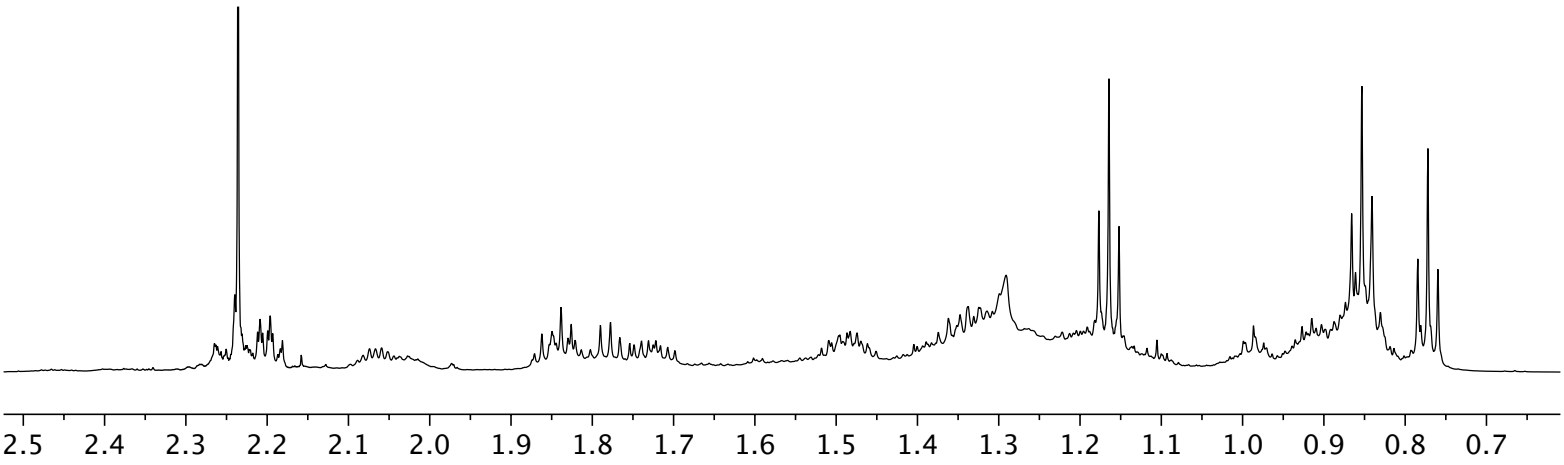

Figure S28. ^{1}H–^{1}H gCOSY (600 MHz) spectrum of gracilioether L in CD_3OD

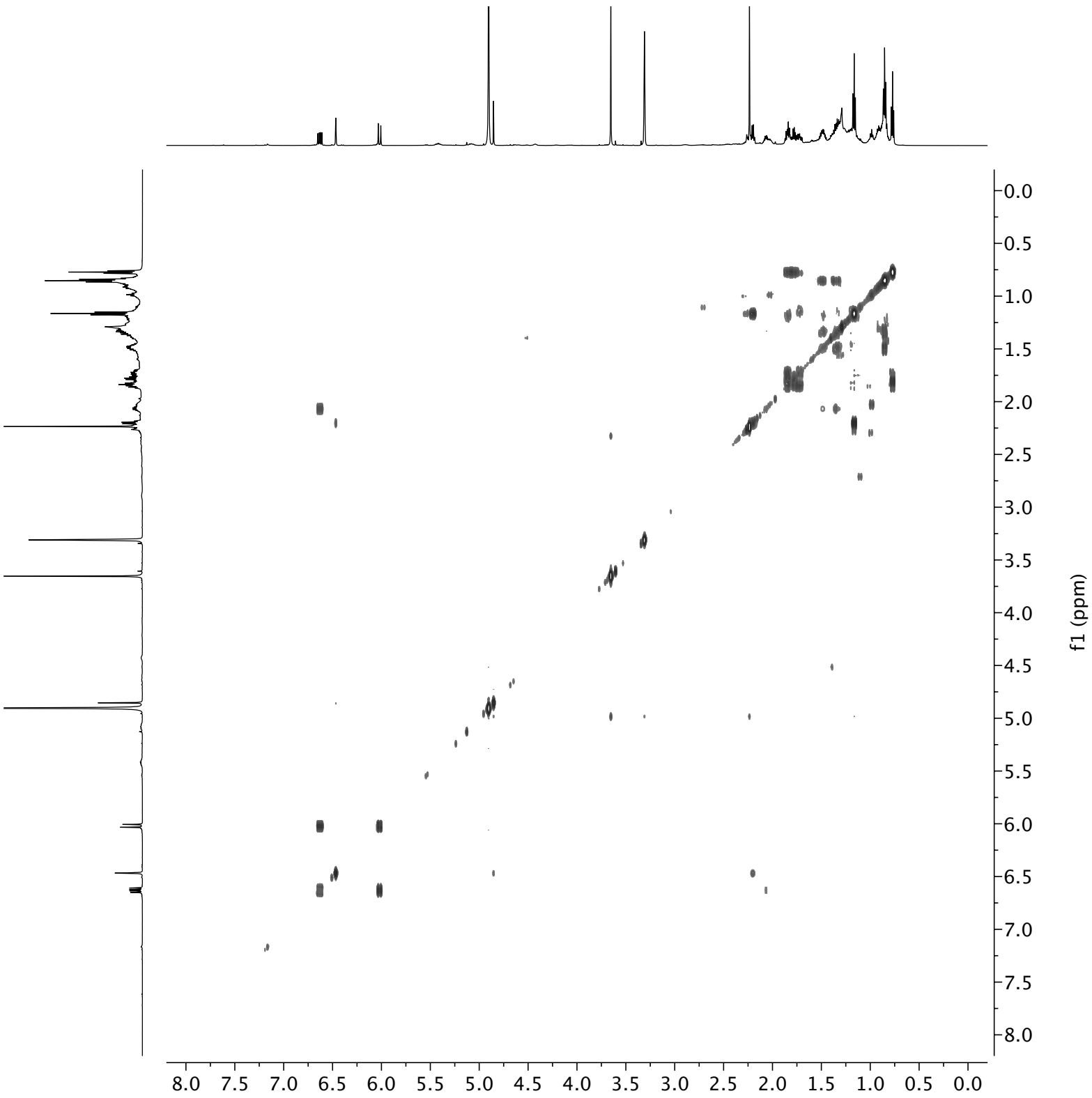

Figure S29. ^{1}H–^{1}H NOESY (600 MHz) spectrum of gracilioether L in CD_3OD

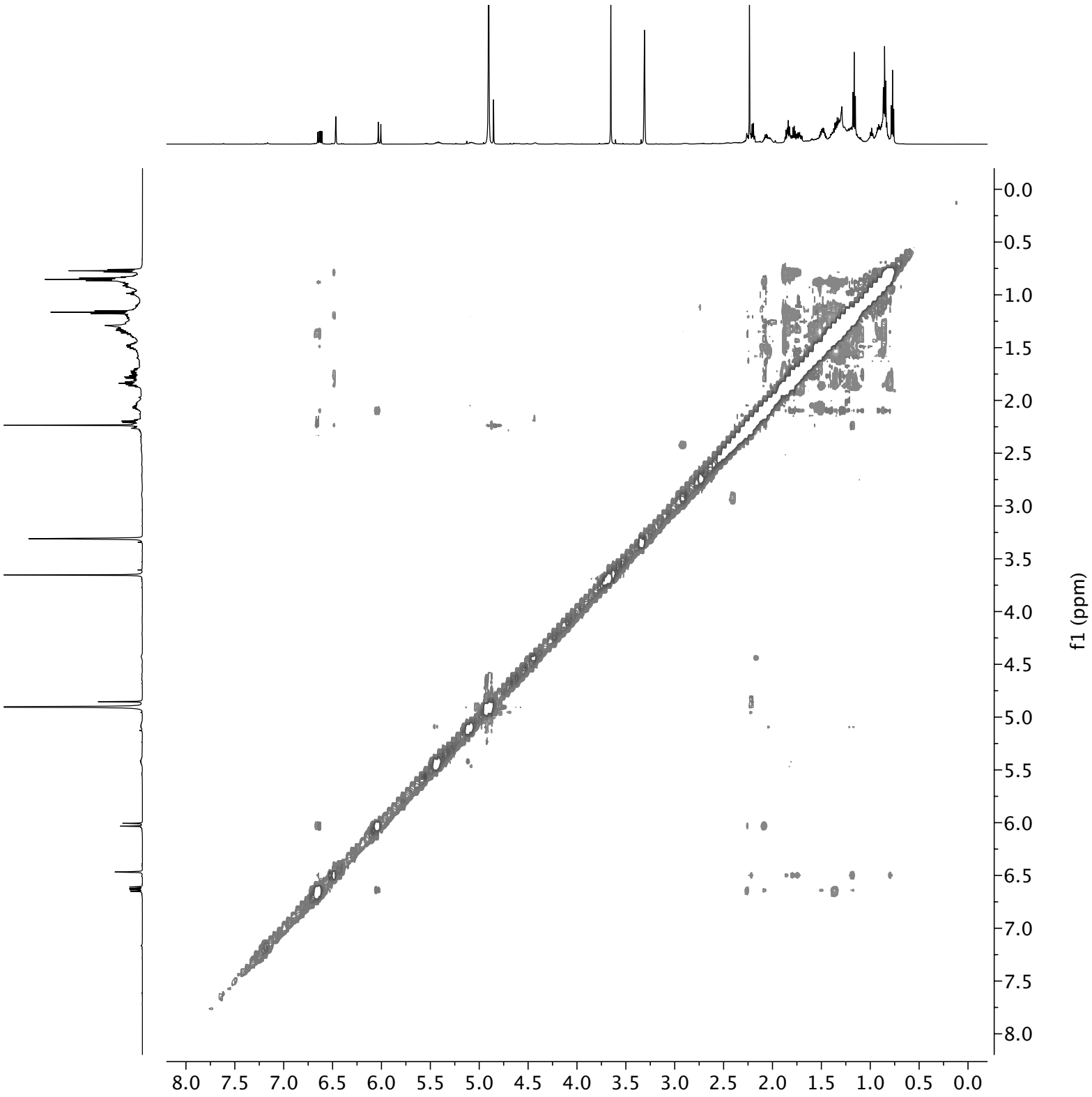

Figure S30. $^{1}H-^{13}C$ HMBC (600 MHz) spectrum of gracilioether L in CD_3OD